Analysis of carbon and nitrogen dynamics in riparian soils: Model development

A. Brovelli [*], J. Batlle-Aguilar [1], D.A. Barry

Ecological Engineering Laboratory, Institute of Environmental Engineering, Faculté de l'Environnement Naturel, Architectural et Construit (ENAC), École Polytechnique Fédérale de Lausanne (EPFL), Station 2, 1015 Lausanne, Switzerland (alessandro.brovelli@epfl.ch andrew.barry@epfl.ch)

[1] *Now at National Centre for Groundwater Research and Training (NCGRT), School of the Environment, Flinders University, GPO Box 2100, Adelaide, South Australia 5001, Australia. Email:* jordi.batlleaguilar@flinders.edu.au

Accepted for publication in *Science of the Total Environment*,

9 April 2012

* Corresponding author, ph.: +41 (0) 21 693 59 19, fax: +41 (0) 21 693 80 35

Abstract

The quality of riparian soils and their ability to buffer contaminant releases to aquifers and streams are connected intimately to moisture content and nutrient dynamics, in particular of carbon (C) and nitrogen (N). A multi-compartment model – named the Riparian Soil Model (RSM) – was developed to help investigate the influence and importance of environmental parameters, climatic factors and management practices on soil ecosystem functioning in riparian areas. The model improves existing tools, in particular regarding its capability to simulate a wide range of temporal scales, from days to centuries, along with its ability to predict the concentration and vertical distribution of dissolved organic matter (DOM). It was found that DOM concentration controls the amount of soil organic matter (SOM) stored in the soil as well as the respiration rate. The moisture content was computed using a detailed water budget approach, assuming that within each time step all the water above field capacity drains to the layer underneath, until it becomes fully saturated. A mass balance approach was also used for nutrient transport, whereas the biogeochemical reaction network was developed as an extension of an existing C and N turnover model. Temperature changes across the soil profile were simulated analytically, assuming periodic temperature changes in the topsoil. To verify the consistency of model predictions and to illustrate its capabilities, a synthetic but realistic soil profile in a deciduous forest was simulated. Model parameters were taken from the literature, and model predictions were consistent with experimental observations for a similar scenario. Modelling results stressed the importance of environmental conditions on SOM cycling in soils. The mineral and organic C and N stocks fluctuate at different time scales in response to oscillations in climatic conditions and vegetation inputs/uptake.

Keywords

Ecohydrology, nutrient dynamics, soil restoration, soil organic matter, RECORD project, numerical modeling, water budget

Notation

SYMBOL	PARAMETER DESCRIPTION	DIMENSIONS
A	Amplitude of the temperature fluctuations	[ºC]
a	Maximum litter input rate (seasonal component)	$[ML^{-2}T^{-1}]$
$a^{\pm}$	Relative mobility of inorganic nitrogen	[-]
ADD	Total litter input rate	$[ML^{-2}T^{-1}]$
b	Time at which litter is added at the maximum rate	[T]
BD	Biomass decay rate	$[ML^{-3}T^{-1}]$
BIO	Biomass uptake rate of DOM (dissolved organic matter)	$[ML^{-3}T^{-1}]$
c	Width of the added litter Gaussian function	[T]
C_b	Soil carbon biomass pool	$[ML^{-3}]$
C_b^{max}	Soil microbial carrying capacity	$[ML^{-3}]$
C_d	Soil dissolved carbon pool	$[ML^{-3}]$
C_h	Soil carbon humus pool	$[ML^{-3}]$
C_l	Soil carbon litter pool	$[ML^{-3}]$
C_{CO_2}	Inorganic carbon pool	$[ML^{-3}]$
DEC_h	C leaving the humus pool due to microbial decomposition	$[ML^{-3}T^{-1}]$
DEC_l	C leaving the litter pool due to microbial decomposition	$[ML^{-3}T^{-1}]$
$DENIT$	Denitrification rate	$[ML^{-3}T^{-1}]$
E	Evapotranspiration rate	$[LT^{-1}]$
E_w	Evapotranspiration rate at the wilting point	$[LT^{-1}]$
E_p	Potential evapotranspiration rate	$[LT^{-1}]$
$f_d(s)$	Activity coefficient accounting for the soil moisture effects on decomposition	[-]
$f_{dn}(s)$	Dimensionless activity coefficient describing the effect of soil moisture on denitrification	[-]
$f_n(s)$	Dimensionless activity coefficient describing the effect of	[-]

	soil moisture on nitrification	
$f_p(t)$	Coefficient describing the seasonal variation of plant activity	[-]
F	Dimensionless parameter	[-]
H(·)	Heaviside step function	[-]
H_{CF}	Thickness of the capillary fringe	[L]
i	Soil compartment index	[-]
I	Infiltration rate	[LT^{-1}]
I_b	Biomass inhibition factor	[-]
I_c	Canopy interception rate	[LT^{-1}]
$IMM^{\pm}$	Nitrate and ammonium immobilization rate	[$ML^{-3}T^{-1}$]
IMM_{DOM}	Potential immobilization rate of dissolved organic matter	[$ML^{-3}T^{-1}$]
IMM_{MAX}	Maximum total (immobile and dissolved) immobilization rate	[$ML^{-3}T^{-1}$]
IMM_{SOM}	Potential immobilization rate of immobile organic matter	[$ML^{-3}T^{-1}$]
k_h	First-order humus decomposition rate	[$L^3T^{-1}M^{-1}$]
k_l	First-order litter decomposition rate	[$L^3T^{-1}M^{-1}$]
k^+	First-order ammonium immobilization rate	[$L^3T^{-1}M^{-1}$]
k^-	First-order nitrate immobilization rate	[$L^3T^{-1}M^{-1}$]
$k_{m,h}$	First-order rate for humus mobilisation	[T^{-1}]
$k_{m,l}$	First-order rate for litter mobilisation	[T^{-1}]
k_d	First-order microbial death rate	[T^{-1}]
k_{DC}	Rate of dissolved carbon returning to the biomass pool	[$L^3M^{-1}T^{-1}$]
k_{dn}	First-order denitrification rate	[T^{-1}]
k_n	Nitrification rate constant	[T^{-1}]
L	Leakage rate	[LT^{-1}]
MIN	Mineralization rate	[$ML^{-3}T^{-1}$]
MOB_h	Dissolution rate of C_b	[$ML^{-3}T^{-1}$]
MOB_l	Dissolution rate of C_l	[$ML^{-3}T^{-1}$]

n	Soil porosity	[-]
N^+	Soil ammonium pool	[ML^{-3}]
N^-	Soil nitrate pool	[ML^{-3}]
NIT	Nitrification rate	[$ML^{-3}T^{-1}$]
N_b	Soil nitrogen biomass pool	[ML^{-3}]
N_d	Soil nitrogen dissolved pool	[ML^{-3}]
N_g	Nitrogen gases (N_2 and N_2O) resulting from denitrification	[ML^{-3}]
N_h	Soil nitrogen humus pool	[ML^{-3}]
N_l	Soil nitrogen litter pool	[ML^{-3}]
$_p$	Nutrient pool index (litter, humus, biomass)	[-]
P	Precipitation rate	[LT^{-1}]
P_c	Total rainfall reaching the soil surface after canopy interception	[LT^{-1}]
q_{tv}	Maximum amount of water that can infiltrate to the aquifer within one time step	[L]
r	Rate of litter addition (constant component)	[$ML^{-2}T^{-1}$]
r_h	Fraction of decomposed C going into the humus pool	[-]
r_r	Fraction of decomposed C going into respiration	[-]
RE	Root exudates production rate	[$ML^{-3}T^{-1}$]
RE^{max}	Maximum root exudates production rate	[$ML^{-3}T^{-1}$]
R	Runoff rate	[LT^{-1}]
s	Water saturation	[-]
s^*	Soil moisture level of incipient stress	[-]
s_{CF}	Soil water content in the capillary fringe	[-]
s_{fc}	Soil water content at field capacity	[-]
s_h	Soil moisture level at the hygroscopic point	[-]
s_w	Soil moisture level at wilting point	[-]
t	Time	[T]
T	Temperature	[°C]

T_d^{max}	Temperature at which the maximum decomposition rate is attained	[°C]
U	Soil water content above field capacity that can move downward by gravity	[L]
$UP^{\pm}$	Total nitrate and ammonium plant uptake rate	[$ML^{-3}T^{-1}$]
$UP_a^{\pm}$	Nitrate and ammonium active uptake rate	[$ML^{-3}T^{-1}$]
$UP_p^{\pm}$	Nitrate and ammonium passive uptake rate	[$ML^{-3}T^{-1}$]
V	Soil compartment storage capacity	[L]
v_d	Spread of the temperature-activity function	[°C]
Z	Soil compartment thickness	[L]
α	Mean rainfall depth	[L]
φ	Non-dimensional factor accounting for possible reduction of the decomposition rate when SOM is poor in N	[-]
γ	Non-dimensional inhibition factor to reduce the DOM uptake rate when the pore water is poor in N	[-]
λ	Rainfall frequency	[T^{-1}]
λ_h	Thermal conductivity	[$WL^{-1}K^{-1}$]
Φ	Net N transfer from/to nitrogen mineral pools	[$ML^{-3}T^{-1}$]
Γ	Net N transfer among mineral N pools and DOM	[$ML^{-3}T^{-1}$]
$(C/N)_{add}$	C:N ratio of added organic matter	[-]
$(C/N)_b$	C:N ratio of biomass pool	[-]
$(C/N)_d$	C:N ratio of dissolved pool	[-]
$(C/N)_h$	C:N ratio of humus pool	[-]
$(C/N)_l$	C:N ratio of litter pool	[-]

1

2

1. Introduction

Sustainable management of riparian soils is of primary importance to preserve natural ecosystem functioning. Riparian zones are sources of ecosystem functions and services including biodiversity hotspots, water quality enhancement, and recreation sites (Brinson et al., 1981; Naiman and Decamps, 1997). Throughout the world, the ecological condition of natural riparian systems has declined due to a number of factors, including streamflow regulation, floodplain development, channelization, and the spread of non-native species (Naiman and Decamps, 1997; Naiman et al., 2005). Consequently, restoration of riparian areas has become a global management priority (Hughes et al., 2005; Hughes and Rood, 2003; Webb and Erskine, 2003).

Soil ecosystem functioning is connected intimately to soil organic matter (SOM) turnover, a set of complex and intertwined biological processes that recycle biotic residues (such as plant litter, dead organisms, etc.) to inorganic molecules. Environmental and climatic factors affect decomposition rates, the biological activity of the soil and ultimately SOM cycling (Laio et al., 2001; Porporato et al., 2003). Soil moisture has a direct influence on the processes mediated by the soil biota (pedofauna, bacteria, fungi, etc.) because optimal decomposition rates are achieved only in a narrow saturation range (Bell et al., 2008; Ju et al., 2006; Porporato et al., 2003; Van Gestel et al., 1992). Owing to the strong dependence of ecological processes on soil moisture, linear and non-linear interactions and feedbacks exist between hydrological processes and soil ecosystem functioning (Curiel Yuste et al., 2007; Misson et al., 2005; Scott-Denton et al., 2006; Van Gestel et al., 1993), with rainfall and temperature fluctuations being the major external forcing factors of the climate-soil-vegetation system (Davidson and Janssens, 2006; Gu et al., 2004; Porporato and D'Odorico, 2004; Rodriguez-Iturbe et al., 1999). Changes in precipitation characteristics affect the release of soluble OM components to the pore water (Park and Matzner, 2003; Sanderman et al., 2008), and therefore potentially modify nutrient cycling, soil functioning and carbon stocks in organic horizons (Fröberg et al., 2008). The amount, quality and distribution of DOM has an important ecological significance (Kalbitz and Kaiser, 2003), and understanding its dynamics is of critical importance for studying and predicting the functioning of soil ecosystems, rates of weathering and contaminant release (e.g., Kalbitz et al., 2003; Kalbitz et al., 2000;

Marschner and Kalbitz, 2003). Variations in the climatic conditions – for example, the future increase of extreme precipitation events foreseen by many meteorological models (e.g., Trenberth et al., 2003) – will impact SOM stocks, possibly contributing to increase green-house gases release – i.e., CO_2 and N_2O – and to decrease soil fertility.

A second crucial external forcing factor for SOM and soil productivity – related to vegetation rather than to climate – is the amount and quality of the litter input (Dent et al., 2006; Elliott et al., 1993; Manzoni et al., 2008; Paul et al., 2001; Sørensen, 1974). In particular, the C to N ratio (C/N) of the added litter is a very sensitive parameter. The importance of freshly deposited litter on soil activity was confirmed in a number of recent studies measuring CO_2 production (Rasmussen et al., 2007; 2008). In a laboratory experiment, Crow et al. (2009) found that doubling the litter input accelerated soil respiration in an unpredictable manner. It was proposed that the unexpected increase was related to the additional nutrient availability in the pore solution. This finding has implications for the long-term soil nutrient balance because it suggests that the increased plant productivity might deplete soil C stocks rather than contribute to CO_2 sequestration. Litter input rates and their temporal patterns are modified following a change in soil use: As a consequence, the C and N stocks, soil fertility and DOM dynamics are altered in manner that is difficult to predict (Batlle-Aguilar et al., 2011; Chantigny, 2003; Kalbitz et al., 2000).

To summarize, numerous experimental observations have highlighted the importance of SOM changes at multiple time scales, from daily to inter-annual. The distribution of the soil C and N immobile stocks in different horizons and the dissolved organic matter (DOM) dynamics are important for understanding soil quality and functioning, and to foresee possible variation in nutrient turnover following a change in ecosystem management. The goal of this work was to develop a numerical tool able to simulate SOM turnover in riparian soils with natural or semi-natural vegetation (grassland or forest). The developed model can be used to improve and facilitate the design of restoration schemes.

2. Model development

The model is based on the assumptions that the soil profile being studied can be sub-divided in a number of functional units – named layers or compartments – and that within each layer the soil is homogeneous. The number of layers used in the existing simulators is variable, from batch (one compartment) to more

complicated multi-layer models ranging from 2 to 6 compartments (Botter et al., 2006; Daly et al., 2008; Garnier et al., 2001; Hansen et al., 1991; Jenkinson and Coleman, 2008; Porporato et al., 2003) and to finely discretized meshes (e.g., PASTIS model, Lafolie, 1991). Previous works have shown that, depending on the complexity of the soil, the optimal number of compartments is between 4 and 10, such as in the RothC (Jenkinson and Coleman, 2008; Jenkinson and Rayner, 1977), CENTURY (Kirschbaum and Paul, 2002; Parton et al., 1987) and IBIS (Kucharik et al., 2000) models. The soil nutrient dynamics simulator presented in the following, named the Riparian Soil Model (RSM), is one-dimensional and multi-compartment. The mathematical description of nutrient turnover is an extended version of the biogeochemical reaction network used in many existing simulators, such as the CENTURY and RothC models (Jenkinson et al., 1990; Jenkinson and Coleman, 2008; Parton et al., 1987). To introduce the RSM, the same terminology and notation used recently by Porporato et al. (2003) is adopted. The main features of the simulator are depicted in Fig. 1 and can be summarized as follows:

- Soil profile discretisation. The RSM considers a soil profile composed of four different functional units found in riparian soils. The units represent (i) the topsoil, a shallow layer rich in freshly deposited SOM, (ii) the root zone, where most of the biological transformations take place and nutrients and water are available for plants, (iii) the parent material (or bedrock), the deep mineral horizon scarcely modified by pedogenetic processes, and (iv) the aquifer, the lowermost layer that remains permanently water-saturated and where oxygen availability is diffusion-limited. For each compartment, the physical properties (porosity, thickness, water holding capacity, etc.) and the biological transformation rates can be assigned independently. Evapotranspiration and plant nutrient uptake were limited to the two shallower compartments where roots are present.
- Water and solute transport. The moisture content of each compartment was computed using a water-budget approach, described in detail in Par. 2.1. The moisture dynamics are controlled by climate – precipitation, evapotranspiration – and by the physical properties of the soil substrate, e.g., water holding capacity and aquifer dynamics. The soluble SOM fraction and the inorganic dissolved N are transported with water from one compartment to its neighbour. It was assumed that each compartment is well mixed and that the concentrations are uniform.

- Temperature. Heat flux and soil temperature changes along the profile were modelled assuming a periodic temperature forcing function for the topsoil. The average temperature in each compartment was computed using the analytical solution for a semi-infinite profile, presented in Par. 2.2.
- Nutrient pools. Eight nutrient pools were considered: Four SOM fractions, three of which are immobile – litter, humus, biomass – and one mobile (organic matter dissolved in the pore solution, DOM), two mineral N species, nitrate and ammonia. Furthermore, inorganic C (i.e., CO_2) and N gases (N_2 and N_2O) were accounted for as additional state variables (or nutrient pools), owing to the fact that gas efflux is frequently measured (e.g. Bell et al., 2008; Crow et al., 2009) during studies of soil biogeochemistry to estimate soil respiration and denitrification rates.
- Vegetation. Vegetation exerts a large influence on soil water budget, is a major source of soil C and N through litterfall, affects DOM dynamics via root exudates, varies temporally over seasonal or intra-annual periods, and modifies inorganic nitrogen availability. The model considers these feedbacks on nutrient dynamics.
- Biochemical transformations. The biological reaction network includes microbial respiration of the mobile and immobile pools, mobilization and immobilization of DOM, root release of labile OM and microbiological uptake from the pore solution. In addition, the N cycle involves mineralization of organic N, nitrification and denitrification processes. Details and mathematical description of the reaction network are given in Par. 2.3.

The model was implemented using Matlab (http://www.mathworks.com/). The total simulation time was divided into discrete time steps. The length of each step should be selected based on the typical time scale at which hydrological processes happen in the simulated system. For example, the typical time scale for flow in sandy-loamy soils is 1 d (Hefting et al., 2005; Kirschbaum, 1999). This value was used in the simulations reported here, while for a coarser material (e.g., sandy gravel) a smaller time step would be required, as coarse materials drain faster. During each time step, the water balance equation for the four compartments is solved and the saturation level of each compartment at the end of the step and the net water fluxes are computed. Within each time step, the ordinary differential equations describing solute transport and reactions (presented in Par. 2.2) are numerically integrated using a 4^{th}-5^{th} order Runge-Kutta scheme with adaptive time stepping. To compute the biological coefficients that depend on soil moisture content, it was assumed

that water saturation varies linearly within each time step, with the initial and final saturation computed from the water flow sub-module. Note that the word 'pool' is used in this manuscript to represent the soil C and N groups with similar characteristics within the nutrient turnover and transport sub-model, while the word 'compartment' is used to denote the soil layer.

2.1 Moisture dynamics

Soil compartments fill and drain in response to hydrologic processes. Richards' (and Darcy's) equation is often used to describe water transport in variably saturated soil profiles (Garnier et al., 2001; Hansen et al., 1991; Liu et al., 2005; Maggi and Porporato, 2007). However, while Richards' equation is suitable to model unsaturated flow in laboratory-scale soil columns with limited heterogeneity, its applicability to field-scale studies, where local scale variability is significant, has been debated (Dekker and Ritsema, 1994; Flury et al., 1994; Ritsema, 1999; Steenhuis et al., 1996). At the field scale, unsaturated flow is often governed by the heterogeneous distribution of the hydraulic properties, soil water repellence, instability and preferential flow paths (Lennartz et al., 2008; Morales et al., 2010; Ritsema and Dekker, 2000). Preferential flow paths are created in a number of intertwined factors related to climate, pedofauna, vegetation and soil management practices, including soil cracks during wetting/drying cycles, dead roots and earthworm channels (Angers and Caron, 1998), and result in rapid penetration of water from the topsoil to deeper horizons. An alternative approach to model moisture changes in the soil profile is the water budget approach, accounting for infiltration and evapotranspiration, leakage to the aquifer and run-off (Barry et al., 1983; Parton et al., 1987; Porporato et al., 2003; Rose et al., 1982). Neighbouring compartments are hydraulically connected, and water transport is driven by gravity. The water budget approach, although simplified, if properly tuned is a suitable practical means to represent the soil moisture dynamics of the upper part of the soil profile rather than computationally intensive numerical schemes based on solutions of Richards' equation (Kim et al., 1996; Struthers et al., 2006).

The model is made up of four compartments: the three shallower are variably saturated, while the deeper compartment represents an unconfined aquifer (i.e., it is permanently water-filled), with constant water elevation controlled by the regional hydraulic gradient (Fig. 1). Near riverbanks, the water saturation of the entire soil profile can be influenced by groundwater dynamics triggered by fluctuations of the river elevation.

In the model, piezometric data can be used to define the saturation of each compartment. At each time step, each layer is checked to determine whether its centre is within the saturated zone or the capillary fringe (defined by a user-specified thickness H_{cf} [m]). In this case, the water saturation of the compartment is set to unity (for the saturated zone) or to the user-defined saturation of the capillary fringe (s_{cf} [-]). The properties of the capillary fringe can be estimated from the characteristic retention curve of the soil. Following Rose et al. (1982), Barry et al. (1983) and Parton et al. (1987), it was assumed that within one time step the excess of water above field capacity drains to the compartment underneath, if it has enough storage capacity. The water balance of compartment *i* (with *i* = 1, 2, 3) is given by

$$\Delta s_i = \frac{I_i(s,t) - E_i(s,t) - L_i(s,t)}{n_i Z_i} \Delta t, \tag{1}$$

where $s_i(t)$ [-] is water saturation ($0 \le s_i(t) \le 1$), n_i is porosity [-], Z_i is the compartment thickness [L], and $I_i(s, t)$, $E_i(s, t)$, $L_i(s, t)$ are, respectively, the infiltration, evapotranspiration and leakage rates [L T^{-1}].

Infiltration in compartments 2 and 3 is equivalent to the leakage from the compartment above (i.e., $I_i(s,t) = L_{i-1}(s,t), i = 2,3$). Instead, for the topsoil, the infiltration rate was computed from rainfall intensity and the amount of rainfall that can infiltrate within one time step as limited by the storage capacity.

In the simulations presented in this work, synthetic time series of precipitation were randomly generated employing the methodology presented in Laio et al. (2001). Rainfall occurrence is described by a Poisson process with frequency λ [T^{-1}], while rainfall depths follow an exponential distribution with mean α [L]. Measured precipitation sequences could also be used, or alternative approaches (which, for example, consider lagged correlation) could be implemented to produce precipitation time series. The rainfall reaching the soil surface, P_c, is equal to the rainfall depth reduced by the canopy interception, $P_c = \max(0, P - I_C)$. Rainfall interception by plant canopies is defined using an exponential relationship, $I_C = \gamma\left[1 - \exp(-\delta P)\right]$, where γ [L] and δ [L^{-1}] are empirical parameters, which depend on the vegetation characteristics and climate (Calder, 1993).

Evapotranspiration, $E(s,t)$, represents the combined losses by plant transpiration and soil evaporation and occurs only in shallow horizons where roots are present. In the model, it was assumed that roots develop only in the first and second compartments, that is, the topsoil and the root zone. The actual evapotranspiration is a function of the soil saturation, and was computed as (Laio et al., 2001):

$$E(s,t)=\begin{cases} E_w \dfrac{s(t)-s_h}{s_w-s_h}, & s_h < s(t) \le s_{w,} \\ E_w + \left(E_p - E_w\right)\dfrac{s(t)-s_w}{s^*-s_w}, & s_w < s\left(t\right) \le s^*, \\ E_p, & s^* < s\left(t\right) \le 1, \end{cases} \tag{2}$$

where s_w [-] is the wilting point (saturation level at which plant transpiration halts due to very low levels of soil moisture), s_h [-] is the hygroscopic point (water molecules are strongly bound to the soil matrix and they are not available for plants), s^* [-] is the soil moisture of incipient stress (level below which plants start reducing transpiration by closing their stomata to prevent internal water losses), E_p and E_w [L T^{-1}] are, respectively, the potential evapotranspiration rate and the rate at wilting point. Potential evapotranspiration is dependent on temperature,

$$E_p(T) = \mathrm{H}(T)\, g T^{l} \tag{3}$$

where H(·) is the Heaviside step function (Abramowitz and Stegun, 1972), g [L T^{-1} C^{-1}] and l [-] two empirical parameters that depend on vegetation, soil and climate characteristics (Xu and Singh, 2001). Actual evapotranspiration is equal to the maximum value, E_p, when soil saturation is close to unity, then $E(s,t)$ decreases linearly until the wilting point. For moisture contents below s_w, only evaporation is active, and the water loss rate reduces linearly from E_w to zero at the point of hygroscopic water, s_h.

Leakage losses are driven by gravity. For each compartment, within a time step, all the water above field capacity (U, [L]) can move downward, unless the storage capacity of the compartment underneath, V [L], is exceeded:

$$L_i(s,t) = \frac{\min\left[U_i(s,t), V_{i+1}\left(s, t+\frac{1}{2}\right)\right]}{\Delta t}, \tag{4}$$

$$U_i = H\left[s_i(t) - s_{fc}\right]\left[s_i(t) - s_{fc}\right] n_i Z_i, \tag{5}$$

$$V_i(s,t) = \left[1 - s_i\left(t+\frac{1}{2}\right)\right] n_i Z_i, \tag{6}$$

where s_{fc} is the soil field capacity, and $s(t + 1/2)$ indicates the water saturation after the losses due to leakage and evapotranspiration. In practice, evapotranspiration and potential leakage rates are first computed for compartments 1 to 3 using the initial saturation. Next, the potential leakage is reduced in case the receiving compartment becomes fully saturated, and the excess water increases the local soil water content. When the topsoil becomes fully saturated, additional water cannot infiltrate and precipitation is converted to runoff. The runoff rate, $R(t)$ [L T^{-1}] is given by:

$$R(t) = \frac{H\left[P_c(t)\Delta t - V_1\left(s, t+\frac{1}{2}\right)\right]\left[P_c(t)\Delta t - V_1\left(s, t+\frac{1}{2}\right)\right]}{\Delta t}. \tag{7}$$

Some care is required to compute the effective leakage from compartment 3 to the aquifer. The model uses a threshold value, q_{tv}, to define the maximum amount of water that can infiltrate into the aquifer within one time step, and therefore Eq. (3) for compartment 3 becomes $L_3(s,t) = \min\left[U_3(s,t), q_{tv}\Delta t\right]/\Delta t$. Note that q_{tv} controls the average soil water content of the profile. The dimensionless parameter F can be used to define whether leakage or infiltration dominate the soil moisture dynamics,

$$F = \frac{\langle P\rangle - \langle E\rangle}{q_{tv}}, \tag{8}$$

where $\langle\ \rangle$ indicates the average daily precipitation and evapotranspiration. Three regimes can be identified, as illustrated in Fig. 2. Panel (a) shows the average monthly rainfall used in this example, with two wet

(spring and fall) and two dry (summer and winter) seasons. Panels (b), (c) and (d) instead report the moisture content during one year in the top soil, root zone and parent material for three conditions. When $F \gg 1$, net infiltration is larger than the leakage rate and the soil profile is permanently water-saturated. This often occurs because the geological layer below the soil is poorly permeable, and leads to the formation of wet regions were SOM accumulates (e.g., bogs, peatlands). In the second extreme case, $F \ll 1$, the soil profile drains quickly and water saturation is seldom above field capacity. This situation is typical of immature sandy soils and recently deposited sediments poor in organic matter (Bharati et al., 2002; Radke and Berry, 1993). In the third, intermediate, case, $F \approx 1$, the soil moisture is sensitive to the climatic conditions, and shows inter-annual variability depending on the actual precipitation rate.

2.2 Temperature dynamics

Heat transport along a soil profile is proportional to the temperature gradient, while convective heat transport resulting from water movement can in most cases be neglected (Jury and Horton, 2004; Roth, 2007). This approximation is valid in particular for soils that remain always partially wet, as is the case for riparian areas. In most situations, the temperature of the soil surface (soil/air interface) can be represented as a linear combination of periodic signals:

$$T\left(0,t\right) = T_0 + \sum_{i=1}^{n} A_i \sin(\omega_i t), \tag{9}$$

with $1 \le n \le 3$ (for example, seasonal and daily fluctuations). Using Eq. 9 as the boundary condition, the heat transport equation can be solved analytically, and the temperature at an arbitrary depth z can be computed for a semi-infinite profile as (Jury and Horton, 2004; Roth, 2007):

$$T\left(z,t\right) = T_0 + \sum_{i=1}^{n} A_i \sin(\omega_i t - k_i z)\exp\left(-k_i z\right), \tag{10}$$

where $k_i = \sqrt{\omega_i / 2D_h}$ [L^{-1}] is the wave number, $D_h = \lambda_h / C_h$ [$L^2\ T^{-1}$] is the effective thermal diffusivity, λ_h and C_h the effective thermal conductivity and thermal capacity of the soil. Eq. (10) is used in the model to compute the soil temperature in each layer (at the centre of the compartment) at each time step, with the

bulk thermal capacity computed as $C_h = (1-\phi)C_g + \phi(1-s_{fc})C_a + \phi s_{fc} C_w$, where C_w, C_g, C_a are the thermal capacities of water, solid grains and air, respectively. An example of temperature changes along a hypothetical soil profile is shown in Fig. 3. The topsoil temperature (black line) oscillates at two scales ($n = 2$ in Eq. 9), daily and seasonal. At increasing depths – 50 and 100 cm, root zone and parent material (red and blue lines) – the high frequency fluctuations quickly disappear, the seasonal oscillations are progressively damped and the phase shift increases.

2.3 Solute transport and nutrient turnover

The SOM reaction network is an extended version of the soil C and N turnover model of Porporato et al. (2003), coupled with mass-balance for solute transport. Eight pools are considered in the RSM model: four for SOM (immobile litter, humus and microbial biomass and dissolved organic matter, DOM), inorganic C (i.e., CO_2) and three for inorganic N (ammonium, nitrate and N gas, i.e., denitrification products, N_2 and N_2O). In terms of processes, abiotic mobilization (dissolution) of SOM, biomass consumption of DOM and denitrification were consequently added to the transformation network. Following Porporato et al. (2003), all the biological reactions were modelled using a first-order kinetic rate, which represents an average transformation rate. This approach, although approximate, has been used often to study nutrient cycles in soil systems (Paul and Clark, 1996) because it reduces the number of parameters and facilitates model calibration. DOM (both C and N), ammonium and nitrate are the mobile components. Their transport within the soil profile follows the water infiltration and leakage among neighbouring compartments. Within each soil compartment, full mixing was assumed. Upward movement (for example due to ploughing, bioturbation or capillary raise) was ignored. To facilitate the comparison with experimental data, the model was designed so that the soil content of immobile components was computed using units of mass per unit volume of soil, while units of mass per unit volume of pore solution (i.e., concentration in the pore fluid) were used for the mobile components (DOM and mineral N pools).

2.3.1 Soil carbon

The model assumes that fresh litter is deposited in the first and second compartments, although with a different rate (typically, the rate of addition is larger in the topsoil). Sources of fresh litter are vegetation residues (leaves, branches, stems, roots, etc.) and dead pedofauna. Dead organic C pools – fresh litter and

partially decomposed humus – are oxidized and dissolve in the pore water. Fig. 4 depicts the overall C turnover network. Note that notation consistent with that of Porporato et al. (2003) is used in the following equations. For the same reason, nutrient fluxes among compartments are defined in terms of mass per unit time per unit volume. The transformation rates of the three immobile organic C fractions for each compartment (subscript *i*) are given by:

$$\frac{dC_{l,i}}{dt} = \frac{ADD_i}{Z_i} + BD_i - DEC_{l,i} - MOB_{l,i}, \tag{11}$$

$$\frac{dC_{h,i}}{dt} = r_h DEC_{l,i} - DEC_{h,i} - MOB_{h,i}, \tag{12}$$

$$\frac{dC_{b,i}}{dt} = \left(1 - r_h - r_r\right) DEC_{l,i} + \left(1 - r_r\right)\left(DEC_{h,i} + BIO_i\right) - BD_i, \tag{13}$$

where C_l, C_h and C_b are the C concentrations in the litter, humus and biomass pools, respectively [M L^{-3}], *ADD* is the litter input rate [M L^{-2} T^{-1}], *BD* is the biomass decay rate [M L^{-3} T^{-1}], DEC_l and DEC_h are, respectively, the C fluxes leaving the litter and humus pools due to microbial decomposition [M L^{-3} T^{-1}], MOB_l, MOB_h are, respectively, the dissolution rates of litter and humus pools [M L^{-3} T^{-1}], and *BIO* is the biomass uptake rate of DOM [M L^{-3} T^{-1}]. Finally, r_h and r_r are non-dimensional coefficients representing the transformation efficiency, i.e., the fractions of decomposed C that goes into the humus pool and to respiration, respectively. Note that the litter input rate *ADD* was always set to zero in the deep compartments, parent material and aquifer. Following Porporato et al. (2003), SOM microbial decomposition rates are modelled using first-order kinetics:

$$DEC_p = \varphi f_d^s(s)\, f_d^T(T)\, k_p I_B C_b C_p, \tag{14}$$

where the subscript *p* indicates the corresponding pool (*p* = *l*, *h* for litter or humus, respectively), the coefficient φ [-] is a non-dimensional factor that accounts for a possible reduction of the decomposition rate when the SOM is poor in N and the N immobilization is not sufficient to integrate the N required by the bacteria (see Par. 2.2.4 for details), k_p [L^3 T^{-1} M^{-1}] is the first-order decomposition rate, computed as a

weighted average of the rates of the different organic molecules that form the pool and $f_d^s(s)$ and $f_d^T(T)$ [-] are two activity coefficients accounting for the soil moisture and temperature effects on decomposition (Benbi and Richter, 2002; Davidson et al., 1998; Porporato et al., 2003):

$$f_d^s(s) = \begin{cases} \dfrac{s}{s_{fc}}, s \le s_{fc,} \\ \dfrac{s_{fc}}{s}, s > s_{fc}, \end{cases} \tag{15}$$

$$f_d^T(T) = \exp\left[-\frac{\left(T - T_d^{max}\right)^2}{2v_d^2} \right]. \tag{16}$$

The shape of the two relationships is illustrated in Fig. 6. Panel (a) shows the influence of moisture content while (b) that of temperature. The temperature dependency of the microbial reactions (Eq. 15) is expressed using a Gaussian curve, a typical response for reactions controlled by enzymatic activity: T_d^{max} is the temperature at which the largest decomposition rate is attained, and v_d is the spread of the function. A typical value for T_d^{max} is around 25 ºC, whereas v_d is a measure of the sensitivity to temperature changes: respiration of different C pools exhibits different sensitivity (Davidson and Janssens, 2006; Gu et al., 2004). The term I_b [-] is an inhibition factor that was introduced to define the largest biomass population that the soil can sustain. This parameter is often named carrying capacity (Odum and Barrett, 2005), and it is defined as (e.g., Barry et al., 2002; Brovelli et al., 2009):

$$I_b = \frac{C_b^{max} - C_b}{C_b^{max}}, \tag{17}$$

where C_b^{max} [M L^{-3}] is the maximum permitted biomass concentration. The inhibition factor defined by Eq. (13) accounts for all the possible mechanisms that limit biomass growth not explicitly included in the model, such as the scarcity of nutrients other than N (e.g., P, S, etc.) or their reduced availability within the bio-phase as their transport becomes limited by diffusion. The carrying capacity of the ecosystem was not

considered in the original formulation of Porporato et al. (2003) but it is crucial to obtain realistic modelling results in environments rich in nutrients where water is also abundant.

The biomass decay rate BD is computed as in Porporato et al. (2003), $BD = k_d C_b$, where k_d is the first-order rate of microbial lysis [T^{-1}]. A first-order rate was also used to model abiotic SOM dissolution (MOB_l and MOB_h) and biomass uptake rates:

$$MOB_l = k_{m,l} m_l C_l, \tag{18}$$

$$MOB_h = k_{m,h} m_h C_h, \tag{19}$$

$$BIO = \gamma f_d^w(s)\, f_d^T(T)\, k_{DC} I_B C_d C_b, \tag{20}$$

where $k_{c,l}$ and $k_{c,h}$ [T^{-1}] are first-order rates of litter and humus mobilization, k_{DC} [$M\ L^{-3}\ T^{-1}$] is the rate of dissolved C returning to the biomass pool, and γ [-] is a non-dimensional inhibition factor to reduce the DOM uptake rate when the pore water is poor in N (see Par. 2.2.4). The dissolution of SOM is a kinetically controlled process, and only a fraction of the available litter and humus is soluble in water at ambient temperature (Gregorich et al., 2003; Kalbitz et al., 2000; Marschner and Kalbitz, 2003). Two parameters, m_l and m_h [-], were therefore introduced to specify the fraction of litter and humus that can dissolve within the time scale considered in the simulations. The mobilization rate instead should be computed as the average of the slow and fast SOM pools weighted by their relative abundance. It has been reported that microbial enzymes can foster SOM dissolution rates (Kalbitz et al., 2000; Marschner and Kalbitz, 2003): This process was not explicitly included in the model, but can be accounted for by increasing the mobilization rates. In addition to litter and humus dissolution and mobilization, root exudates also contribute to labile DOM content of soils. Organic compounds released from roots play a number of extremely important roles for plant physiology, such as protection from environmental stresses (drought, parasites, toxic compounds, e.g., metals), or plant-plant and plant-microbe communication (Rovira, 1969; Walker et al., 2003).The rates of root exudates production are extremely variable and depend on environmental and climatic factors. In experiments, it has been found that typically a fraction in the range 5-20% of the total photosynthesized C is released to the rhyzosphere as exudates (Walker et al., 2003; Yano et al., 2000). Owing to the important

ecological role of root exudates, their temporal dynamics are tightly linked to plant physiology and health and, more specifically, plants produce abundant root exudates when photosynthetic processes are active (Curiel Yuste et al., 2007; Rovira, 1969). Following (Gu et al., 2003; 2008), a plant activity function $f_p(t), 0 \le f_p(t) \le 1$ was defined:

$$f_p(t) = \frac{1}{1+\exp\left[-(t-d_1)/b_1\right]} - \frac{1}{1+\exp\left[-(t-d_2)/b_2\right]}, \quad (21)$$

with empirical coefficients b_1, b_2, d_1, d_2 [T] that mimic the seasonal patterns of canopy photosynthetic activity. The actual rate of plant-derived DOC was modelled as:

$$RE_i(t) = RE_i^{max} f_p(t), \quad (22)$$

where RE_i^{max} [M L^{-3} T^{-1}] is the maximum root exudation rate, a function of vegetation type and density. The influence of moisture content on the production of exudates is instead neglected. This is motivated by previous findings (Rovira, 1969; Walker et al., 2003) that have shown that exudate production reduces only when the moisture content falls below the wilting point, a condition that is observed rarely in riparian areas. On the other hand, in waterlogged soils or during flood events plant physiology can be influenced negatively. The effect on root exudates production is, however, unclear and is certainly limited in flood-tolerant species that are commonly found along riverbanks (Rovira, 1969; Walker et al., 2003).

The total dissolved C of each soil compartment was computed combining all the above-mentioned processes,

$$\frac{dC_{d,i}}{dt} = \frac{\left(MOB_{l,i} + MOB_{h,i} + RE_i - BIO_i\right) Z_i + L_{i-1} C_{d,i-1} - L_i C_{d,i}}{s_i n_i Z_i}. \quad (23)$$

DOC in rainwater is normally very low relative to soil porewaters, and therefore negligible concentrations are present in infiltrating rainwater in the first compartment ($C_{d,0} = 0$). In other conditions, however, for example during a flood, the water infiltrating into the soil profile can be rich in DOM, as accounted for in the model.

During OM degradation and decomposition, CO_2 is generated. Since respiration is frequently measured in soil field studies, the model was designed to compute inorganic C production from each compartment,

$$\frac{dC_{CO_{2,i}}}{dt} = r_r \left(DEC_{l,i} + DEC_{h,i} + BIO_i \right). \tag{24}$$

2.3.2 Soil organic nitrogen

The turnover of organic N in the mobile and immobile OM pools corresponds to the C balance equations scaled by the appropriate C/N ratio (Fig. 5), and is computed as:

$$\frac{dN_{l,i}}{dt} = \frac{ADD_i}{Z_i \left(C/N\right)_{add,i}} + \frac{BD_i}{\left(C/N\right)_{b,i}} - \frac{DEC_{l,i}}{\left(C/N\right)_{l,i}} - \frac{MOB_{l,i}}{\left(C/N\right)_{l,i}}, \tag{25}$$

$$\frac{dN_{h,i}}{dt} = r_h \frac{DEC_{l,i}}{\left(C/N\right)_{h,i}} - \frac{DEC_{h,i}}{\left(C/N\right)_{h,i}} - \frac{MOB_{h,i}}{\left(C/N\right)_{h,i}}, \tag{26}$$

$$\frac{dN_{b,i}}{dt} = \left[1 - r_h \frac{\left(C/N\right)_{l,i}}{\left(C/N\right)_{h,i}} \right] \frac{DEC_{l,i}}{\left(C/N\right)_{l,i}} + \frac{DEC_{h,i}}{\left(C/N\right)_{h,i}} + \frac{BIO}{\left(C/N\right)_{d,i}} - \frac{BD_i}{\left(C/N\right)_{b,i}} - \Phi_i - \Gamma_i \ , \tag{27}$$

$$\frac{dN_{d,i}}{dt} = \frac{\left[\frac{MOB_{l,i}}{(C/N)_{l,i}} + \frac{MOB_{h,i}}{(C/N)_{h,i}} + \frac{RE_i}{(C/N)_r} - \frac{BIO}{(C/N)_{b,i}} \right] Z_i + L_{i-1} N_{d,i-1} - L_i N_{d,i}}{s_i n_i Z_i}, \tag{28}$$

where N_l, N_h and N_b [M L^{-3}] are, respectively, the N concentrations in the litter, humus and biomass pools, $(C/N)_{add}$, $(C/N)_l$, $(C/N)_h$, $(C/N)_b$, $(C/N)_d$ and $(C/N)_r$ [-] are, respectively, the C:N ratios of added organic matter, litter, humus, biomass, dissolved organic pools and root exudates, Φ and Γ are N sources/sinks from the mineral pools (nitrate and ammonia) and are relevant to the immobile SOM and to the DOM, respectively. The physical meaning of the terms Φ and Γ is discussed in detail in Par. 2.2.4.

2.3.3 Soil inorganic nitrogen

Inorganic N (ammonium, N^+ and nitrate, N^-, [M L^{-3}]) concentrations result from the balance between transport, mineralization and immobilization. Immobilization occurs when the OM (immobile and/or

dissolved) is poor in N, $(C/N)_{bio} > (C/N)_{OM}$, while mineralization takes place if there is an N surplus, $(C/N)_{bio} < (C/N)_{OM}$ (Porporato et al., 2003). For each compartment, the inorganic N pools and N gases (N_2 and N_2O), N_g, were computed as:

$$\frac{dN_i^+}{dt} = \frac{L_{i-1}a^+N_{i-1}^+ - L_i a^+ N_i^+ + (MIN_i - UP_i^+ - NIT_i - IMM_i^+ - IMM_{d,i}^+)Z_i}{s_i n_i Z_i}, \quad (29)$$

$$\frac{dN_i^-}{dt} = \frac{L_{i-1}a^-N_{i-1}^- - L_i a^- N_i^- + (NIT_i - UP_i^- - IMM_i^- - IMM_{d,i}^- + MIN_i - DENIT_i)Z_i}{s_i n_i Z_i}, \quad (30)$$

$$\frac{dN_{g,i}}{dt} = DENIT_i, \quad (31)$$

where $UP^{\pm}$ are the plant N uptake rates [M L^{-3} T^{-1}], MIN is the mineralization rate [M L^{-3} T^{-1}], $IMM^{\pm}$ are the immobilization rates [M L^{-3} T^{-1}], NIT and $DENIT$ [M L^{-3} T^{-1}] are the nitrification and denitrification rates, respectively. The dimensionless coefficients $a^{\pm}$ ($0 \le a^{\pm} \le 1$) are the mobile fractions of ammonium and nitrate: Since ammonium is strongly adsorbed onto the soil clays, it is assumed that nitrate is mobile ($a^- = 1$) while ammonium is not ($a^+ \approx 0.1$) (Porporato et al., 2003). Consequently, only a small fraction of ammonia can reach the deep horizons, while nitrate easily reaches the watertable (unless it is removed by denitrification).

Plant N uptake is a complex process, and not understood completely. A similar approach to that of Porporato et al. (2003) was adopted, which is outlined briefly. The approach assumed that the total uptake rate $UP^{\pm}$ is a linear combination of two processes, passive $(UP_p^{\pm})$ and active $(UP_p^{\pm})$ uptake. Passive uptake is a function of plant transpiration, and reduces as the soil dries. Active uptake is closely related to the plant metabolic processes: The plant compensates for the N deficit by pumping the N available from the pore solution to the roots. Active uptake is a function of both soil moisture content and availability of inorganic N near the roots. If N is not available (or has already been taken up), the process halts. The total plant uptake is computed as the sum of the passive and active terms, this latter scaled by the plant seasonal activity coefficient (Eq. 21),

$UP^{\pm} = UP_p^{\pm} + f_p(t)UP_a^{\pm}$. The scaling parameter f_p is introduced to account for the reduction in nutrient uptake in periods where the vegetation metabolic activity is reduced.

In riparian zones, the primary mechanisms of nitrate removal are denitrification (conversion to gaseous forms of N) and plant uptake (Hill et al., 2000), whereas NH_4^+ typically undergoes oxidation to NO_3 and plant uptake (Lorah et al., 2009). Nitrification and denitrification rates are modelled as first-order processes (Heinen, 2006; Porporato et al., 2003), but unlike the model presented by Porporato et al. (2003), the dependence on carbon biomass is neglected:

$$NIT = k_n f_n^s(s) f_n^T(T) N^+, \tag{32}$$

$$DENIT = k_{dn} f_{dn}^s(s) f_{dn}^T(T) N^-, \tag{33}$$

where k_n [T^{-1}] is the nitrification rate, $f_n^s(s)$ and $f_n^T(T)$ are dimensionless activity coefficients describing the effect of soil moisture and temperature on ammonium transformation, k_{dn} [T^{-1}], $f_{dn}^s(s)$ and $f_{dn}^T(T)$ are the first-order rate, soil saturation and temperature activity coefficients for denitrification. Discarding the dependence of nitrification and denitrification rates from biomass is equivalent to assuming that (i) the transformations involving inorganic N pools only are performed by microbial consortia different from the heterotrophs and (ii) that the rates are only weakly sensitive to changes in biomass density compared to other sources of variability. This second assumption is valid because the moisture content (and, ultimately, oxygen availability) is the key environmental controlling factor (Arah and Vinten, 1995; Heinen, 2006; Paul and Clark, 1996). The first assumption is justified for nitrification because nitrifying bacteria are chemoautotrophs and use CO_2 as a carbon source (Paul and Clark, 1996). Instead, microorganisms using nitrate as an electron acceptor are mainly heterotrophic, but only a (relatively small) fraction of the total soil biomass population is able to reduce nitrates (Paul and Clark, 1996). It is therefore reasonable to neglect the correlation between nitrification rate and carbon biomass.

Temperature variations of nitrification and denitrification rates were modelled using the same function applied to decomposition Eq. (15), although coefficients can be different. Moisture dependency of nitrification was instead modelled as:

$$f_n(s) = \begin{cases} \dfrac{s}{s_{fc}}, & if\ s \le s_{fc}, \\ \dfrac{1-s}{1-s_{fc}}, & if\ s > s_{fc}. \end{cases} \quad (34)$$

While nitrification reaches an optimal value near field capacity, and decreases as the water content increases to saturation (Fig. 6a), denitrification shows contrasting behaviour. In fact, nitrification consumes the oxygen dissolved in the pore solution, and so oxygen availability becomes diffusion-limited as saturation increases. Denitrification instead occurs in anoxic (reducing) conditions and therefore the denitrification rate approaches a maximum as the soil profile becomes fully saturated. Oxygen diffusion coefficients are non-linear in relation to the air-filled pore space, so a steep non-linear relationship is used for the water content reduction function (Grundmann and Rolston, 1987; Heinen, 2006), as shown in Fig. 6a:

$$f_{dn}(s) = H(s - s_{fc}) \left(\frac{s - s_{fc}}{1 - s_{fc}} \right)^{\frac{3}{2}}. \quad (35)$$

2.3.4 N mineralization and immobilization

In the model of Porporato et al. (2003), N availability and dynamics control the SOM turnover rate. In particular, the model is designed so that the biomass C/N value remains constant, a necessary condition for life. Therefore, biomass can only grow (i.e., decompose the SOM) if enough N is available to preserve the target C/N. This condition can only be achieved in two cases: (i) the C/N value of the decomposable SOM is equal or larger than that of the biomass, or (ii) mineral N is available and biomass can convert it into organic forms via immobilization. Mineral N pools are formed when the C/N of the SOM is larger than that of the biomass, and therefore N is available in excess. Organic forms of N (for example amino acids, peptides, proteins, etc.) are converted to nitrate and ammonium via mineralization. Therefore, not only the amount of litter added to the soil is an important factor controlling the turnover rate, but also its quality. This will be examined in detail in the next section. Porporato et al. (2003) defined two interrelated variables to reduce the SOM decomposition rate when N is the limiting factor. The first variable, Φ, is the net N flux from/to the mineral pools, i.e., mineralization (*MIN*) or immobilization (*IMM*), $MIN = H(\Phi)\Phi$ and IMM =

$-H\left(-\Phi\right)\Phi$. Note that in the following the subscripts SOM and DOM indicate to which OM pool the immobilization process is relevant. Following Porporato et al. (2003), the Φ parameter is computed to maintain the biomass C/N constant:

$$\frac{d\left(C/N\right)_b}{dt}=\frac{dC_b}{dt}-\frac{dN_b}{dt}\left(C/N\right)_b=0. \tag{36}$$

Eq. (36) is easily solved after combining the biomass C and N balance equations, and leads to an expression that can be used to compute Φ (Porporato et al., 2003). A second variable, φ, is used to reduce the SOM decomposition rate when immobilization is not sufficient to cover the N deficit. N immobilization is a kinetically controlled process, and its rate is defined by mineral N availability, biomass concentration and activity:

$$IMM_{max}=\left(k^{+}N^{+}+k^{-}N^{-}\right)f_d^s\left(s\right)f_d^T\left(T\right)C_b, \tag{37}$$

where k^{+} and k^{-} [$L^3\ T^{-1}\ M^{-1}$] are first-order ammonium and nitrate immobilization rates. When the potential immobilization is larger than the maximum ($IMM_{SOM}>IMM_{max}$), $\varphi<1$ and the decomposition rate is reduced (see Porporato et al., 2003 for details on how this condition is implemented). The original formulation of the model, however, only considers decomposition of the immobile SOM (litter and humus). The model was therefore updated to consider a similar reduction of the biomass uptake from the dissolved organic matter. The net flux among mineral N pools and DOM, Γ, is given by:

$$\Gamma=f_d^s\left(s\right)f_d^T\left(T\right)k_{DC}C_bC_d\left[\frac{1}{\left(C/N\right)_{DC}}-\frac{1-r_r}{\left(C/N\right)_b}\right]. \tag{38}$$

Mineralization again takes place if the net N flux is positive, $MIN_{DOM}=H\left(\Gamma\right)\Gamma$, while immobilization occurs if there is a deficit of N, $IMM_{DOM}=-H\left(-\Gamma\right)\Gamma$. When the dissolved organic pool is deficient in N, $\left(C/N\right)_d<\left(C/N\right)_b$, soil biomass can uptake N from the mineral pools, unless the total immobilization rate exceeds the maximum, $IMM_{SOM}+IMM_{DOM}\le IMM_{max}$. In this case, it is assumed that biomass consumes

preferentially the DOM, since it is more bio-available. A parameter, γ, is used to reduce the biomass uptake of DOM in case the N immobilization is larger than IMM_{max}, i.e., $IMM_{DOM} > IMM_{max}$. In this case, the DOM decomposition reduction factor is computed as:

$$\gamma = -\frac{k^+ N^+ + k^- N^-}{k_{DC} C_d \left[\frac{1}{(C/N)_{DC}} - \frac{1 - r_r}{(C/N)_b} \right]}, \tag{39}$$

while SOM decomposition is halted, i.e., $\varphi = 0$.

As for the SOM pools, immobilization to meet DOM requirements is a linear combination of the nitrate and ammonia mobilization rates, $IMM_{DOM} = IMM^+_{DOM} + IMM^-_{DOM}$:

$$IMM^+_{DOM} = \frac{k^+ N^+}{k^+ N^+ + k^- N^-} IMM_{DOM}, \tag{40}$$

$$IMM^-_{DOM} = \frac{k^- N^-}{k^+ N^+ + k^- N^-} IMM_{DOM}. \tag{41}$$

3. Influence of litter inputs characteristics on soil quality

In this section, a simplified but realistic scenario is presented to illustrate model functioning, to verify its correct implementation, and to ascertain whether modelling assumptions are valid and result in realistic estimates of the soil properties. For this purpose, a base case was set up using parameters taken from the literature and predictions at steady state were compared with the ranges reported in the literature for soils in similar environmental conditions (climate and vegetation characteristics).

3.1 Base case description

All the simulations presented in the following are relevant to a riparian soil in a deciduous forest in a temperate climate (topsoil temperature varied between -5 and 25°C). Rainfall followed a seasonal behaviour, with two wet seasons (spring and fall) and two relatively dry periods (winter and summer), with an average daily rate in the range of 2.25 - 3.75 mm d^{-1}, as shown in Fig. 7. Owing to the high total amount of

precipitation (about 1 m y^{-1} on average), the relatively slow drainage rate ($1 < F < 2$ depending on the season) and the presence of a shallow aquifer (regional watertable at a depth of 1.1 m), soil moisture was seldom a limiting factor for soil biota. The base case was designed to be representative of a structured soil in natural conditions in a riparian zone. Table 1 lists the physical properties of the soil, with the biogeochemical model parameters reported in Table 2, together with the corresponding literature range. Average values were used, except for the first-order SOM dissolution rate. For this parameter, a value close to the lower bound was used to prevent exceedingly high concentrations of dissolved OM in the pore solution.

According to Bell (1978) and Futter et al. (2007), the litter input rates in the topsoil and root zone can be approximated as a combination of two components, a value constant through the year (due, e.g., to macro-fauna, dead roots, etc.) and a seasonal component (i.e., fallen leaves) with a Gaussian density function having its maximum in autumn (around mid-October for the northern hemisphere). The litter inputs in the shallower compartments were therefore computed as:

$$ADD_i(t) = r_i + a_i \exp\left[-\frac{(t-b)^2}{2c^2}\right], 1 \le t \le 365, \quad (42)$$

where t is the day of the year, r_i [gC m^{-2} d^{-1}] is the constant input rate, a_i [gC m^{-2} d^{-1}] is the maximum litter input rate due to fallen leaves, b [d] is the time at which the maximum rate occurs and c [d] the characteristic width of the Gaussian function, which controls the length of the period with significant litter input in the soil from fallen leaves. The litter input rate for the base case is plotted in Fig. 7, and the parameters used in the different scenarios are reported in Table 3. In all the simulations it was assumed that the seasonal component contributed to the topsoil only (i.e., $a_2 = 0$), with input from September to end of November and the maximum around mid-October (b = 285 d and c = 21.6 d), as illustrated in Fig. 7.

3.2 Model predictions for the base case

The model was run to simulate a period of 500 y. Model predictions at steady state were compared with literature values for a comparable soil (similar climate and vegetation). To identify the length scale required for the soil profile to reach steady state conditions, the simulated time series of the soil immobile pools where smoothed using a moving average filter (window of 5 y) and compared with the average values in the

last 50 y. The results are shown in Fig. 8 for the topsoil (panel a, left) and root zone (panel b, right). For the topsoil (Fig. 8a), steady state concentrations are only obtained after about 100 y, whereas in the root zone (Fig. 8a) even after 200 y the litter pool shows large fluctuations, although the mean value remains approximately constant. While the exact value depends on the parameters and initial conditions used, this result suggests that soils reach equilibrium slowly and that if the environmental conditions (for example, climate) change, the effects on soil functioning and nutrient stocks will become evident with a large delay. Model predictions at steady state (average value ±1 standard deviation) are reported in Table 4. The comparison shows that model results fall within the literature ranges for a deciduous forest soil. Since the ranges are rather broad, the satisfactory comparison only indicates that the model captures correctly key processes governing the SOM dynamics in the different compartments. Further comparison with more detailed data was conducted to validate better the fast (i.e., at the daily/monthly time scale) dynamics of OM and was presented elsewhere (Batlle-Aguilar et al., 2012). The main discrepancy between measurements and model predictions concerns the DOM in the root zone, in that the model over-predicts the expected value by a factor of about 2.5. In order to correct this value, the dissolution rate was reduced, and a value close to the lower limit of the range found in the literature was used (Table 2). Indeed, other works (Chantigny, 2003; Kalbitz et al., 2000; Zsolnay, 1996) report values as high as 400 mgC l^{-1} for the average DOC concentration in the upper part of forest soils (organic horizons and root zone), and therefore the model estimate could be regarded as being acceptable. This mismatch however confirms the incomplete knowledge of the mechanisms controlling DOM dynamics and the large uncertainties regarding the dissolution and turnover parameters (Kalbitz et al., 2000; 2003).

The dynamics of the organic and inorganic pools depends on a combination of processes occurring at different time scales, from daily (precipitation occurrence), seasonal (amount of rainfall) to annual (litter input). To understand how the different pools respond to the periodic fluctuations, and to identify the main environmental forcing factors for each pool, the frequency distribution of the simulated time series of concentrations were computed. Spectral analysis of the model results was carried out (MATLAB's FFT function was applied) and the resulting power was normalized using the largest value of each spectrum, so that it was possible to compare the dominant frequencies of each pool and each compartment. Results are reported in Fig. 9 for the topsoil (top panels) and root zone (bottom panels). The left column displays the

power spectra of the immobile C pools, while the column on the right shows the corresponding plot for DOM, CO_2 and denitrification products. The spectra in the Fig. 9 plots reveal that all the pools in all compartments respond at the three dominant frequencies. The processes more sensitive to the seasonal component ($\omega = 0.5\ y^{-1}$) are those that depend on the excess of water in the soil and temperature variations, OM dissolution and denitrification in all the soil layers, followed by respiration in the root zone and parent material. This indicates that during the wet periods, soil becomes waterlogged and consequently respiration slows down while denitrification increases. Immobile C pools and respiration in the topsoil respond strongly at the $1\ y^{-1}$ frequency, i.e., to litter addition in fall. In the deeper horizons, however, only DOM, C biomass and respiration fluctuate at the same time scale, since leaf litter is deposited on the topsoil only. Due to the availability of water (the maximum litter input occurs in a period with high rainfall intensity, see Fig. 7), fresh litter dissolves and is transported to the deeper horizon, where it is consumed by biomass. The soil system also shows fluctuations at much longer time scales, with a period (of the dominant component) of about 100 y for the topsoil, and 60 y for the root zone. Numerical experiments conducted to clarify which process was responsible for these low frequency oscillations showed that they disappear when the litter and humus dissolution rates were decreased to $2 \times 10^{-5}\ d^{-1}$, while they were poorly sensitive to increasing decomposition and lysis rates. In other words, as SOM dissolution became negligible compared to biological decomposition the long wavelength oscillations disappeared. The balance between dissolution and decomposition triggers the long period oscillations. Abiotic dissolution is proportional to the amount of litter and humus in the soil, but also controls the amount of these stocks in two ways: (i) directly, the larger the dissolution the faster immobile SOM pools are reduced, and (ii) indirectly, the decomposition rate is proportional to the concentration of biomass, which – owing to the larger bio-availability of dissolved OM compared to that of litter and humus – is in turn very sensitive to OM concentration in the pore water.

4. Summary and conclusions

Sophisticated numerical models are useful tools to understand the functioning and OM turnover in soils, and ultimately to predict possible changes in soil quality and fertility. Their application, however, requires that values of the key environmental forcing variables – such as precipitation time series and litter input – are reliable. A crucial but very difficult aspect of the application of models to soils is their validation with experimental data. The simulator presented in this work made predictions that agreed well with the ranges

expected from the literature, without calibrating any model parameters. It was however found that the processes governing the dynamics of DOM are still to be clarified in detail, and measurements reported in the literature were not always consistent. This indicates the need to conduct further research on these aspects. The predictions presented here however only indicate that the RSM is able to reproduce long-term variations of the SOM stocks. A more detailed comparison was conducted and is reported by Batlle-Aguilar et al. (2012).

Modelling results stressed the importance of environmental conditions on SOM cycling in soils. The mineral and organic C and N stocks fluctuate at different time scales in response to oscillations in precipitation, temperature and litter input rates, a condition also observed in the field (e.g., Haddad et al., 2002). Most of dominant frequencies in the power spectra of the model predictions were related to climate or vegetation. Low frequency fluctuations with a period of 10-100 y associated with dissolution and decomposition processes were also observed. A sensitivity analysis indicated that these oscillations are controlled by the balance between biological (decomposition) and abiotic (dissolution) processes acting on the immobile SOM stocks. Due to the large number of variables, parameter identification is difficult and small errors in the choice of the more sensitive parameters (primarily the first-order degradation rates) can have a large effect of model results and also affect the time scales associated with the model response (fluctuations of the nutrient pools and time needed to reach steady state). The long time needed to reach steady state raises the question of what is the more suitable initial condition in real applications. In general, this is dictated by the field condition. For a mature, well-developed soil in a stable environment, it is appropriate to use the results obtained after running the model to steady state. On young, undeveloped soils, such as in the case of a gravel/sand bar recently deposited and poorly colonized by vegetation, it would perhaps be more correct to define the initial condition assuming a relatively low OM, mineral N and biomass content.

Acknowledgements

This research is part of the RECORD project of the Competence Centre Environment and Sustainability (CCES, http://www.cces.ethz.ch/projects/nature/Record). Funding has been provided by the Swiss National Science Foundation under grant 200021-113296. The authors wish to thank J. Lüster (WSL – Birmensdorf, Switzerland) for useful discussions, and to the anonymous reviewers for their insightful comments.

References

Abramowitz M, Stegun IA. Handbook of mathematical functions with formulas, graphs, and mathematical tables. New York: Dover Publications, 1972.

Angers DA, Caron J. Plant-induced changes in soil structure: Processes and feedbacks. Biogeochemistry 1998; 42: 55-72. DOI: 10.1023/A:1005944025343.

Arah JRM, Vinten AJA. Simplified models of anoxia and denitrification in aggregated and simple-structured soils. European Journal of Soil Science 1995; 46: 507-517. DOI: 10.1111/j.1365-2389.1995.tb01347.x.

Barry DA, Parlange J-Y, Saffigna PG, Rose CW. Theory of solute transport in soils from the method of characteristics. Irrigation Science 1983; 4: 277-287. DOI:10.1007/BF00389650.

Barry DA, Prommer H, Miller CT, Engesgaard P, Brun A, Zheng C. Modelling the fate of oxidisable organic contaminants in groundwater. Advances in Water Resources 2002; 25: 945-983. DOI:10.1016/s0309-1708(02)00044-1.

Batlle-Aguilar J, Brovelli A, Luster J, Shrestha J, Niklaus PA, Barry DA. Analysis of carbon and nitrogen dynamics in riparian soils. Model validation and sensitivity to environmental controls. Submitted to Science of the Total Environment. 2012.

Batlle-Aguilar J, Brovelli A, Porporato A, Barry DA. Modelling soil carbon and nitrogen cycles during land use change: Review and model application. Agronomy for Sustainable Development 2011; 31: 251-274. DOI:10.1051/agro/2010007

Bell C, McIntyre N, Cox S, Tissue D, Zak J. Soil microbial responses to temporal variations of moisture and temperature in a Chihuahuan desert grassland. Microbial Ecology 2008; 56: 153-167. DOI:10.1007/s00248-007-9333-z.

Bell DT. Dynamics of litter fall, decomposition, and incorporation in the streamside forest ecosystem. Oikos 1978; 30: 76-82.

Benbi D, Richter J. A critical review of some approaches to modelling nitrogen mineralization. Biology and Fertility of Soils 2002; 35: 168-183. DOI: 10.1007/s00374-002-0456-6.

Bharati L, Lee KH, Isenhart TM, Schultz RC. Soil-water infiltration under crops, pasture, and established riparian buffer in Midwestern USA. Agroforestry Systems 2002; 56: 249-257. DOI:10.1023/A:1021344807285.

Botter G, Settin T, Marani M, Rinaldo A. A stochastic model of nitrate transport and cycling at basin scale. Water Resources Research 2006; 42: WR004599. DOI:10.1029/2005WR004599.

Brinson MM, Swift BL, Plantico RC, Barclay JS. Riparian ecosystems: their ecology and status. U.S. Fish and Wildlife Service, Washington, D.C., USA, 1981, pp. 155.

Brovelli A, Malaguerra F, Barry DA. Bioclogging in porous media: Model development and sensitivity to initial conditions. Environmental Modelling & Software 2009; 24: 611-626. DOI:10.1016/j.envsoft.2008.10.001.

Calder IR. Hydrologic effects of land-use change. In: Maidment DR, editor. Handbook of Hydrology. McGraw-Hill, Inc., New York, USA, 1993, pp. 1424.

Chantigny MH. Dissolved and water-extractable organic matter in soils: A review on the influence of land use and management practices. Geoderma 2003; 113: 357-380. DOI:10.1016/s0016-7061(02)00370-1.

Crow SE, Lajtha K, Bowden RD, Yano Y, Brant JB, Caldwell BA, et al. Increased coniferous needle inputs accelerate decomposition of soil carbon in an old-growth forest. Forest Ecology and Management 2009; 258: 2224-2232. DOI: 10.1016/j.foreco.2009.01.014.

Curiel Yuste J, Baldocchi DD, Gershenson A, Goldstein A, Misson L, Wong S. Microbial soil respiration and its dependency on carbon inputs, soil temperature and moisture. Global Change Biology 2007; 13: 2018-2035. DOI:10.1111/j.1365-2486.2007.01415.x.

Daly E, Oishi AC, Porporato A, Katul GG. A stochastic model for daily subsurface CO_2 concentration and related soil respiration. Advances in Water Resources 2008; 31: 987-994. DOI: 10.1016/j.advwatres.2008.04.001.

Davidson EA, Belk E, Boone RD. Soil water content and temperature as independent or confounded factors controlling soil respiration in a temperate mixed hardwood forest. Global Change Biology 1998; 4: 217-227. DOI: 10.1046/j.1365-2486.1998.00128.x.

Davidson EA, Janssens IA. Temperature sensitivity of soil carbon decomposition and feedbacks to climate change. Nature 2006; 440: 165-173. DOI: 10.1038/nature04514.

Dekker LW, Ritsema CJ. Fingered flow: The creator of sand columns in dune and beach sands. Earth Surface Processes and Landforms 1994; 19: 153-164. DOI:10.1002/esp.3290190206.

Dent D, Bagchi R, Robinson D, Majalap-Lee N, Burslem D. Nutrient fluxes via litterfall and leaf litter decomposition vary across a gradient of soil nutrient supply in a lowland tropical rain forest. Plant and Soil 2006; 288: 197-215. DOI: 10.1007/s11104-006-9108-1.

Elliott WM, Elliott NB, Wyman RL. Relative effect of litter and forest type on rate of decomposition. The American Midland Naturalist Journal 1993; 129: 87-95.

Flury M, Flühler H, Jury WA, Leuenberger J. Susceptibility of soils to preferential flow of water: A field study. Water Resources Research 1994; 30: 1945-1954. DOI:10.1029/94wr00871.

Fröberg M, Hanson P, Todd D, Johnson D. Evaluation of effects of sustained decadal precipitation manipulations on soil carbon stocks. Biogeochemistry 2008; 89: 151-161. DOI: 10.1007/s10533-008-9205-8

Futter MN, Butterfield D, Cosby BJ, Dillon PJ, Wade AJ, Whitehead PG. Modeling the mechanisms that control in-stream dissolved organic carbon dynamics in upland and forested catchments. Water Resources Research 2007; 43: W02424. DOI:10.1029/2006wr004960.

Garnier P, Néel C, Mary B, Lafolie F. Evaluation of a nitrogen transport and transformation model in a bare soil. European Journal of Soil Science 2001; 52: 253-268. DOI: 10.1046/j.1365-2389.2001.00374.x

Gregorich EG, Beare MH, Stoklas U, St-Georges P. Biodegradability of soluble organic matter in maize-cropped soils. Geoderma 2003; 113: 237-252. DOI:10.1016/s0016-7061(02)00363-4.

Grundmann GL, Rolston DE. A water function approximation to degree of anaerobiosis associated with denitrification. Soil Science 1987; 144: 437-441.

Gu L, Hanson PJ, Mac Post W, Liu Q. A novel approach for identifying the true temperature sensitivity from soil respiration measurements. Global Biogeochemical Cycles 2008; 22: GB4009. DOI:10.1029/2007GB003164

Gu L, Post WM, Baldocchi D, Andy Black T, Verma SB, Vesala T, et al. Phenology of Vegetation Photosynthesis. In: Schwartz MD, editor. Phenology: An Integrative Environmental Science. 39. Springer Netherlands, 2003, pp. 467-485.

Gu L, Post WM, King AW. Fast labile carbon turnover obscures sensitivity of heterotrophic respiration from soil to temperature: A model analysis. Global Biogeochemical Cycles 2004; 18: GB1022. DOI:10.1029/2003GB002119

Haddad NM, Tilman D, Knops JMH. Long-term oscillations in grassland productivity induced by drought. Ecology Letters 2002; 5: 110-120. DOI: 10.1046/j.1461-0248.2002.00293.x

Hansen S, Jensen HE, Nielsen NE, Svendsen H. Simulation of nitrogen dynamics and biomass production in winter wheat using the Danish simulation model DAISY. Nutrient Cycling in Agroecosystems 1991; 27: 245-259. DOI:10.1007/BF01051131.

Hefting MM, Clement J-C, Bienkowski P, Dowrick D, Guenat C, Butturini A, et al. The role of vegetation and litter in the nitrogen dynamics of riparian buffer zones in Europe. Ecological Engineering 2005; 24: 465-482. DOI: 10.1016/j.ecoleng.2005.01.003.

Heinen M. Simplified denitrification models: Overview and properties. Geoderma 2006; 133: 444-463. DOI:10.1016/j.geoderma.2005.06.010.

Hill AR, Devito KJ, Campagnolo S, Sanmugadas K. Subsurface denitrification in a forest riparian zone: Interactions between hydrology and supplies of nitrate and organic carbon. Biogeochemistry 2000; 51: 193-223. DOI:10.1023/A:1006476514038.

Hughes FMR, Colston A, Mountford JO. Restoring riparian ecosystems: The challenge of accommodating variability and designing restoration trajectories. Ecology and Society 2005; 10: 22pp.

Hughes FMR, Rood SB. Allocation of river flows for restoration of floodplain forest ecosystems: A review of approaches and their applicability in Europe. Environmental Management 2003; 32: 12-33. DOI: 10.1007/s00267-003-2834-8

Jenkinson DS, Andrew SPS, Lynch JM, Goss MJ, Tinker PB. The Turnover of organic carbon and nitrogen in soil. Philosophical Transactions: Biological Sciences 1990; 329: 361-368. DOI: 10.1098/rstb.1990.0177.

Jenkinson DS, Coleman K. The turnover of organic carbon in subsoils. Part 2. Modelling carbon turnover. European Journal of Soil Science 2008; 59: 400-413. DOI:10.1111/j.1365-2389.2008.01026.x.

Jenkinson DS, Rayner JH. The turnover of soil organic matter in some of the Rothamsted classical experiments. Soil Science 1977; 123: 298-305.

Ju W, Jing MC, Black TA, Barr AG, McCaughey H, Rouleet NT. Hydrological effects on carbon cycles of Canada's forests and wetlands. Tellus B 2006; 58: 16-30. DOI:10.1111/j.1600-0889.2005.00168.x.

Jury WA, Horton R. Soil physics. Hoboken, New Jersey: John Wiley & Sons 2004.

Kalbitz K, Kaiser K. Ecological aspects of dissolved organic matter in soils. Geoderma 2003; 113: 177-178. DOI:10.1016/s0016-7061(02)00359-2.

Kalbitz K, Schmerwitz J, Schwesig D, Matzner E. Biodegradation of soil-derived dissolved organic matter as related to its properties. Geoderma 2003; 113: 273-291. DOI:10.1016/S0016-7061(02)00365-8.

Kalbitz K, Solinger S, Park J-H, Michalzik B, Matzner E. Controls on the dynamics of dissolved organic matter in soils: A review. Soil Science 2000; 165: 277-304.

Kim CP, Stricker JNM, Torfs PJJF. An analytical framework for the water budget of the unsaturated zone. Water Resources Research 1996; 32: 3475-3484. DOI:10.1029/95wr02667.

Kirschbaum MUF. CenW, a forest growth model with linked carbon, energy, nutrient and water cycles. Ecological Modelling 1999; 118: 17-59. DOI:10.1016/S0304-3800(99)00020-4.

Kirschbaum MUF, Paul KI. Modelling C and N dynamics in forest soils with a modified version of the CENTURY model. Soil Biology and Biochemistry 2002; 34: 341-354. DOI:10.1016/S0038-0717(01)00189-4.

Kucharik CJ, Foley JA, Delire C, Fisher VA, Coe MT, Lenters JD, et al. Testing the performance of a dynamic global ecosystem model: Water balance, carbon balance, and vegetation structure. Global Biogeochemical Cycles 2000; 14: 795-825. DOI:10.1029/1999GB001138

Lafolie F. Modelling water flow, nitrogen transport and root uptake including physical non-equilibrium and optimization of the root water potential. Nutrient Cycling in Agroecosystems 1991; 27: 215-231. DOI:10.1007/BF01051129.

Laio F, Porporato A, Ridolfi L, Rodriguez-Iturbe I. Plants in water-controlled ecosystems: active role in hydrological processes and response to water stress. II. Probabilistic soil moisture dynamics. Advances in Water Resources 2001; 24: 707-723. DOI:10.1016/S0309-1708(01)00005-7.

Lennartz B, Jarvis N, Stagnitti F. Effects of heterogeneous flow on discharge generation and solute transport. Soil Science 2008; 173: 306-320.

166 Liu J, Price DT, Chen JM. Nitrogen controls on ecosystem carbon sequestration: a model implementation
167 and application to Saskatchewan, Canada. Ecological Modelling 2005; 186: 178-195. DOI:
168 10.1016/j.ecolmodel.2005.01.036.

169 Lorah MM, Cozzarelli IM, Böhlke JK. Biogeochemistry at a wetland sediment-alluvial aquifer interface in a
170 landfill leachate plume. Journal of Contaminant Hydrology 2009; 105: 99-117.
171 DOI:10.1016/j.jconhyd.2008.11.008.

172 Lovett GM, Weathers KC, Arthur MA. Control of nitrogen loss from forested watersheds by soil
173 carbon:Nitrogen ratio and tree species composition. Ecosystems 2002; 5: 712-0718.
174 DOI:10.1007/s10021-002-0153-1.

175 Maggi F, Porporato A. Coupled moisture and microbial dynamics in unsaturated soils. Water Resources
176 Research 2007; 43: WR005367. DOI:10.1029/2006WR005367.

177 Manzoni S, Jackson RB, Trofymow JA, Porporato A. The global stoichiometry of litter nitrogen
178 mineralization. Science 2008; 321: 684-686. DOI: 10.1126/science.1159792.

179 Marschner B, Kalbitz K. Controls of bioavailability and biodegradability of dissolved organic matter in soils.
180 Geoderma 2003; 113: 211-235. DOI:10.1016/s0016-7061(02)00362-2.

181 McClaugherty CA, Pastor J, Aber JD, Melillo JM. Forest litter decomposition in relation to soil nitrogen
182 dynamics and litter quality. Ecology 1985; 66: 266-275.

183 Misson L, Tang J, Xu M, McKay M, Goldstein A. Influences of recovery from clear-cut, climate variability,
184 and thinning on the carbon balance of a young ponderosa pine plantation. Agricultural and Forest
185 Meteorology 2005; 130: 207-222. DOI:10.1016/j.agrformet.2005.04.001.

186 Morales VL, Parlange JY, Steenhuis TS. Are preferential flow paths perpetuated by microbial activity in the
187 soil matrix? A review. Journal of Hydrology 2010; 393: 29-36. DOI:10.1016/j.jhydrol.2009.12.048.

188 Naiman RJ, Decamps H. The ecology of interfaces: Riparian zones. Annual Review of Ecology and
189 Systematics 1997; 28: 621-658. DOI: 10.1146/annurev.ecolsys.28.1.621.

190 Naiman RJ, Decamps H, McClain ME. Riparia: Ecology, conservation, and management of streamside
191 communities. Elsevier Academic Press, San Diego, Calilfornia, USA, 2005, pp. 430.

192 Odum EP, Barrett GW. Fundamentals of ecology. Belmont, California, USA: Thomson Brooks/Cole, 2005.

193 Park JH, Matzner E. Controls on the release of dissolved organic carbon and nitrogen from a deciduous
194 forest floor investigated by manipulations of aboveground litter inputs and water flux.
195 Biogeochemistry 2003; 66: 265-286. DOI: 10.1023/B:BIOG.0000005341.19412.7b

196 Parton WJ, Schimmel DS, Cole CV, Ojima DS. Analysis of factors controlling soil organic matter levels in
197 great plains grasslands. Soil Science Society of the America Journal 1987; 51: 1173-1179.

198 Paul EA, Clark FE. Soil microbiology and biochemistry. San Diego, California, USA: Academic Press,
199 1996.

200 Paul KI, Black AS, Conyers MK. Effect of plant residue return on the development of surface soil pH
201 gradients. Biology and Fertility of Soils 2001; 33: 75-82. DOI: 10.1007/s003740000293.

202 Porporato A, D'Odorico P. Phase transitions driven by state-dependent Poisson noise. Physical Review
203 Letters 2004; 92: 1-4. DOI:10.1103/PhysRevLett.92.110601.

204 Porporato A, D'Odorico P, Laio F, Rodriguez-Iturbe I. Hydrologic controls on soil carbon and nitrogen
205 cycles. I. Modelling scheme. Advances in Water Resources 2003; 26: 45-58. DOI:10.1016/S0309-
206 1708(02)00094-5.

207 Radke JK, Berry EC. Infiltration as a tool for detecting soil changes due to cropping, tillage, and grazing
208 livestock. American Journal of Alternative Agriculture 1993; 8: 164-174. DOI:
209 10.1017/S0889189300005385.

210 Rasmussen C, Southard RJ, Horwath WR. Soil mineralogy affects conifer forest soil carbon source
211 utilization and microbial priming. Soil Science Society of the America Journal 2007; 71: 1141-1150.
212 DOI: 10.2136/sssaj2006.0375.

213 Rasmussen C, Southard RJ, Horwath WR. Litter type and soil minerals control temperate forest soil carbon
214 response to climate change. Global Change Biology 2008; 14: 2064-2080. DOI: 10.1111/j.1365-
215 2486.2008.01639.x

216 Ritsema CJ. Preferential flow of water and solutes in soil. Journal of Hydrology 1999; 215: 1-3.
217 DOI:10.1016/S0022-1694(98)00257-1.

218 Ritsema CJ, Dekker LW. Preferential flow in water repellent sandy soils: Principles and modeling
219 implications. Journal of Hydrology 2000; 231-232: 308-319. DOI:10.1016/S0022-1694(00)00203-1.

220 Rodriguez-Iturbe I, Porporato A, Ridolfi L, Isham V, Cox DR. Probabilistic modelling of water balance at a
221 point: the role of climate, soil and vegetation. Proceedings of the Royal Society of London A 1999;
222 455: 3789-3805. DOI:10.1098/rspa.1999.0477

223 Rose CW, Chichester FW, Williams JR, Ritchie JT. A contribution to simplified models of field solute
224 transport. Journal of Environmental Quality 1982; 11: 146-151.

225 Roth K. Soil Physics Lecture Notes, V1.2. University of Heidelberg, Institute of Environmental Physics,
226 Heidelberg, Germany, 2007, pp. 340.

227 Rovira AD. Plant root exudates. The Botanical Review 1969; 35: 35-57.

228 Sanderman J, Baldock JA, Amundson R. Dissolved organic carbon chemistry and dynamics in contrasting
229 forest and grassland soils. Biogeochemistry 2008; 89: 181-198. DOI: 10.1007/s10533-008-9211-x

230 Scott-Denton LE, Rosenstiel TN, Monson RK. Differential controls by climate and substrate over the
231 heterotrophic and rhizospheric components of soil respiration. Global Change Biology 2006; 12:
232 205-206. DOI:10.111/j.1365-2486.2005.01065.x.

233 Sørensen LH. Rate of decomposition of organic matter in soil as influenced by repeated air drying-rewetting
234 and repeated additions of organic material. Soil Biology and Biochemistry 1974; 6: 287-292. DOI:
235 10.1016/0038-0717(74)90032-7.

236 Steenhuis TS, Ritsema CJ, Dekker LW. Fingered flow in unsaturated flow: From nature to model. Geoderma
237 1996; 70: 83-85. DOI:10.1016/S0016-7061(96)90000-2.

238 Struthers I, Hinz C, Sivapalan M. A multiple wetting front gravitational infiltration and redistribution model
239 for water balance applications. Water Resources Research 2006; 42: W06406.
240 DOI:10.1029/2005wr004645.

241 Tietema A, Boxman AW, Bredemeier M, Emmett BA, Moldan F, Gundersen P, et al. Nitrogen saturation
242 experiments (NITREX) in coniferous forest ecosystems in Europe: a summary of results.
243 Environmental Pollution 1998; 102: 433-437. DOI:10.1016/S0269-7491(98)80065-1.

244 Trenberth, KE, Dai, A, Rasmussen, RM, Parsons, The changing character of precipitation. Bulletin of the
245 American Meteorological Society 2003; 84: 1205-1217. DOI:10.1175/BAMS-84-9-1205.

246 Van Gestel M, Ladd JN, Amato M. Microbial biomass responses to seasonal change and imposed drying
247 regimes at increasing depths of undisturbed topsoil profiles. Soil Biology and Biochemistry 1992;
248 24: 103-111. DOI:10.1016/0038-0717(92)90265-Y.

249 Van Gestel M, Merckx R, Vlassak K. Microbial biomass and activity in soils with fluctuating water contents.
250 Geoderma 1993; 56: 617-626. DOI: 10.1016/0016-7061(93)90140-G.

251 Walker TS, Bais HP, Grotewold E, Vivanco JM. Root exudation and rhizosphere biology. Plant Physiology
252 2003; 132: 44-51. DOI: 10.1104/pp.102.019661.

253 Webb AA, Erskine WD. A practical scientific approach to riparian vegetation rehabilitation in Australia.
254 Journal of Environmental Management 2003; 68: 329-341. DOI: 10.1016/S0301-4797(03)00071-9.

255 Xu CY, Singh VP. Evaluation and generalization of temperature-based methods for calculating evaporation.
256 Hydrological Processes 2001; 15: 305-319. DOI: 10.1002/hyp.119.

257 Yano Y, McDowell WH, Aber JD. Biodegradable dissolved organic carbon in forest soil solution and effects
258 of chronic nitrogen deposition. Soil Biology and Biochemistry 2000; 32: 1743-1751. DOI:
259 10.1016/S0038-0717(00)00092-4.

Zsolnay A. Dissolved humus in soil waters. In: Piccolo A, editor. Humic substances in terrestrial ecosystems. Elsevier, Amsterdam, Netherlands, 1996, pp. 171-223.

Tables

Table 1. Physical and hydraulic parameters of each compartment. The tortuosity index was taken from the literature (Porporato et al., 2003).

Parameter	Units	Topsoil	Root zone	Parent material	Aquifer
Thickness (Z)	m	0.1	0.5	0.5	1.0
Porosity (n)	-	0.45	0.39	0.3	0.25
Field capacity (s_{fc})	-	0.4	0.3	0.25	0.25
Capillary fringe saturation (s_{CF})	-	0.85	0.85	0.85	0.85
Tortuosity index (d)	-	1.5	1.5	1.5	1.5

Table 2. Parameters of the biogeochemical model and their typical ranges. A soil bulk density of 1500 kg m^{-3} was assumed to convert units when appropriate.

Parameter	Units	Value	Typical range	Sources
k_l	$m^3\ d^{-1}\ gC^{-1}$	2.5×10^{-5}	$2 \times 10^{-4} – 5 \times 10^{-6}$	Paul and Clark (1996), Sumner (2000), D'Odorico et al. (2003), Hefting et al. (2005)
k_h	$m^3\ d^{-1}\ gC^{-1}$	2.5×10^{-5}	$2 \times 10^{-4} – 5 \times 10^{-6}$	
k_d	d^{-1}	6.5×10^{-3}	$10^{-1} – 10^{-3}$	
B_{max}	$gC\ m^{-3}$	4000	$5 \times 10^{2} – 5 \times 10^{3}$	Paul and Clark (1996)
$k_{m,l}$	d^{-1}	10^{-3}	$5 \times 10^{-1} – 10^{-4}$	Gödde et al. (1996), Chantigny (2003), Gregorich et al. (2003), Bengtson and Bengtsson (2007)
$k_{m,h}$	d^{-1}	10^{-3}	$5 \times 10^{-1} – 10^{-4}$	
k_{DC}	$m^3\ d^{-1}\ gC^{-1}$	5×10^{-4}	$10^{-2} – 10^{-6}$	
C/N_{bio}	-	11.5	4 – 15	Paul and Clark (1996), D'Odorico et al. (2003)
r_r	-	0.5	0.1 – 0.6	
r_h	-	0.25	0.1 – 0.4	Jenkinson et al. (1990), D'Odorico et al. (2003), Nesme et al. (2005)
k_n	d^{-1}	0.6	0.45 – 7.5	Sumner (2000), D'Odorico et al. (2003)
k_{dn}	d^{-1}	0.1	$10^{-3} – 1$	Sumner (2000), Heinen (2006)

Table 3. Litter input quality and quantity for the scenarios considered. The input rates and C/N ratios are typical for a deciduous forest soil in a temperate climate, with vegetation composed of, for example, oak, maple, beach and elms (Lovett et al., 2002; McClaugherty et al., 1985; Tietema et al., 1998).

Case	Litter input rate (g m^{-2})			C/N_{add}	
	a_1	r_1	r_2	Topsoil	Root zone
Base case	15	1.5	1.5	20	20
A	15	3.0	3.0	20	20
B	15	3.0	3.0	15	30
C	25	2.5	2.5	15	30
D*	15	1.5	1.5	20	20
E	15	3.0	3.0	25	35
V1	2.5	1.0	1.0	20	20
V2	2.5	1.0	1.0	25	35

* Same litter parameters of case A. The initial concentrations of the mineral N pools were different.

278

279 **Table 4.** Model results (base case) and typical values in a temperate climate.

Property	Model predictions	Typical range	Units	Sources
Bacteria, topsoil	2886.1 ± 10.7	500 – 3000 *	gC m^{-3}	Paul and Clark (1996)
Bacteria, root zone	572.4 ± 10.7	50 – 1000 *	gC m^{-3}	Paul and Clark (1996)
C	1.34 ± 0.03	1 – 9	× 10^4 g m^{-3}	Paul and Clark (1996)
C/N	18.81 ± 0.03	18 – 25	-	Paul and Clark (1996)
CO_2 efflux	5.24 ± 0.53	0.5 – 5	g m^{-2} d^{-1}	Borken et al. (1999)
DOC, topsoil	293.3 ± 141.9	50 – 300	mgC l^{-1}	Borken et al. (1999), Kalbitz et al. (2000), Fröberg et al. (2003), Glatzel et al. (2003), Yano et al. (2004)
DOC, root zone	97.0 ± 18.8	5 – 70	mgC l^{-1}	
NH_4-N	2.7± 0.14	0.1 – 7.3	gNH_4-N m^{-2} d^{-1}	Breuer et al. (2002)
NH_4-N	33.4 ± 1.2	27.5 ± 12.9	% of total N	Paul and Clark (1996)
N gaseous loss	2.5 ± 0.3	0 – 30	% of total N	Paul and Clark (1996)

280 * Converted from cell g_{soil}^{-1} to gC m_{soil}^{-3} assuming 0.2 × 10^{-12} gC $cell^{-1}$ (Bratbak and Dundas 1984; Norland et

281 al., 1987) and a soil bulk density of 1500 kg m^{-3}

Figure captions

Fig. 1. Conceptual representation of the soil profile used in the model. The soil was subdivided into four functional units (compartments), each considered to be homogeneous. A mass-balance approach is used for the water and solute exchange among the compartments.

Fig. 2. Change in moisture content in different soil compartments as a function of F and the illustrated precipitation. The dimensionless parameter F indicates whether infiltration or leakage dominates the soil moisture dynamics. Panel (a) shows the precipitation regime considered, while panels (b) to (d) report the moisture content in the three shallower compartments. Depending on F, the soil is permanently saturated ($F \gg 1$), drained ($F \ll 1$) or the moisture content fluctuates following the amount of precipitation ($F \approx 1$).

Fig. 3. Simulated temperature changes in the three variably saturated compartments. High frequency fluctuations are damped in the deep layers, and a phase shift appears. The signal propagation from the topsoil is controlled by heat diffusivity, which in turn depends on soil porosity and moisture content.

Fig. 4. Overview of the C turnover model. Arrows show the direction of C transfer, solid lines are transfers within the soil profile, and dashed lines show import and export from the given compartment. The same reaction network is used for each compartment.

Fig. 5. Soil N turnover model for compartment *i*. Arrows show the direction of N transfer, solid lines are transfers within the soil profile, and dashed lines show import and export from the given compartment. The thick dashed line divides the organic and inorganic N pools.

Fig. 6. Activity of different soil biomass consortia as a function of water saturation (Panel a): heterotrophs (f_d), nitrifiers (f_n) and denitrifiers (f_{dn}). These functions were used in Eqs. 11, 16, 26 and 27. The right panel (b) shows the function used to account for the influence of temperature on microbial transformations.

Fig. 7. Litter input rate in the topsoil from a temperate deciduous forest (dashed blue line) and mean daily rainfall for the period considered (solid line, green). The litter input rate is relevant to the base case (Table 3). The average precipitation rate was smoothed using a moving average with a window size of 20 d.

Fig. 8. Time required to reach the steady-state concentration of litter, humus and biomass content in the topsoil (a) and root zone (b). The concentration time series are smoothed using a moving average with a window of 5 y, and divided by the average concentration at steady state (after 500 y) to compute the relative distance from steady state. This is reached after about 80-100 y. Only results at the steady state (t > 100 y) were considered for the following plots.

Fig. 9. Normalised power spectra for selected C and N pools in the first compartment (top panels) and root zone (bottom panels). In the topsoil, litter input ($\omega = 1\ y^{-1}$) and precipitation (season behaviour, $\omega = 0.5\ y^{-1}$) dominate the spectra of all pools. On the contrary, seasonal and annual fluctuations dominate in the root zone, and the low frequency fluctuations (the maximum power occurs with a period of about 60 y) are observed for all the immobile C pools. While in the topsoil the dynamics of litter is dominated by litter fall, in the root zone the same pool is more sensitive to dissolution and decomposition, the two processes responsible for the low frequency oscillations.

Figures

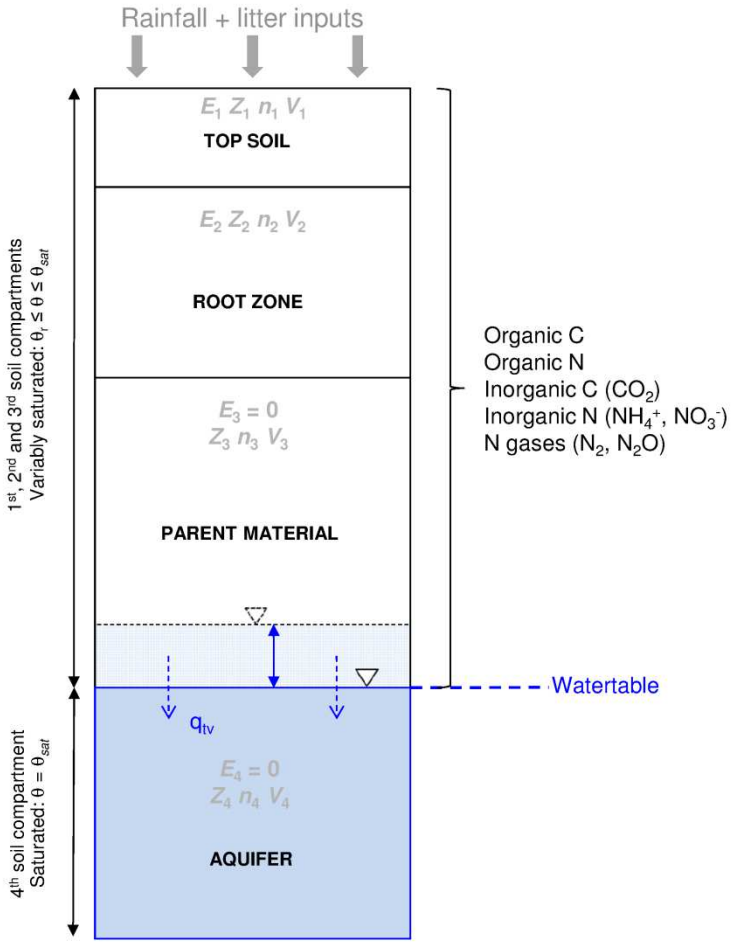

Fig. 1

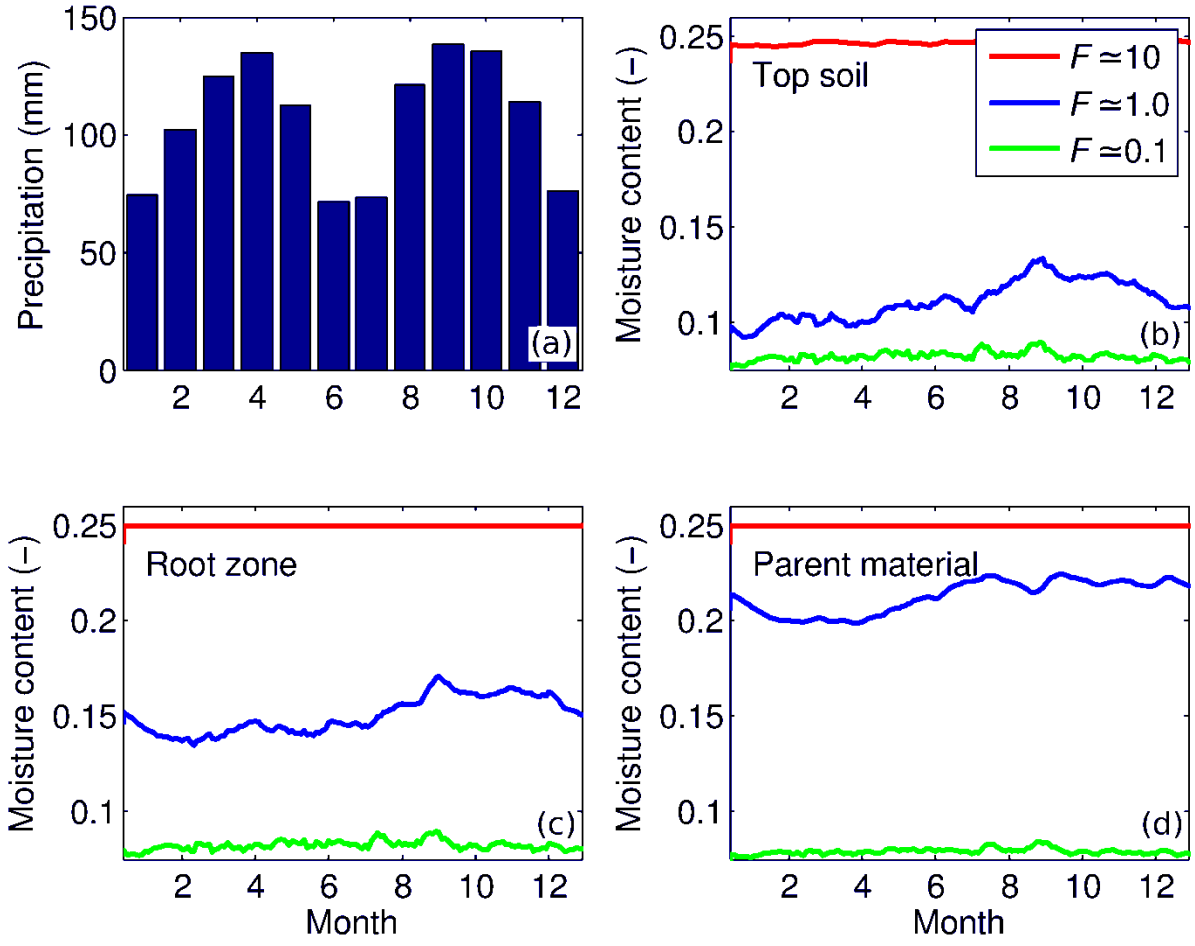
Precipitation (mm)
150
100
50
0
2
4
6
8
10
12
(a)
Moisture content (–)
0.25
0.2
0.15
0.1
Top soil
F ≃10
F ≃1.0
F ≃0.1
(b)
Root zone
(c)
Parent material
(d)
Month

Fig. 2.

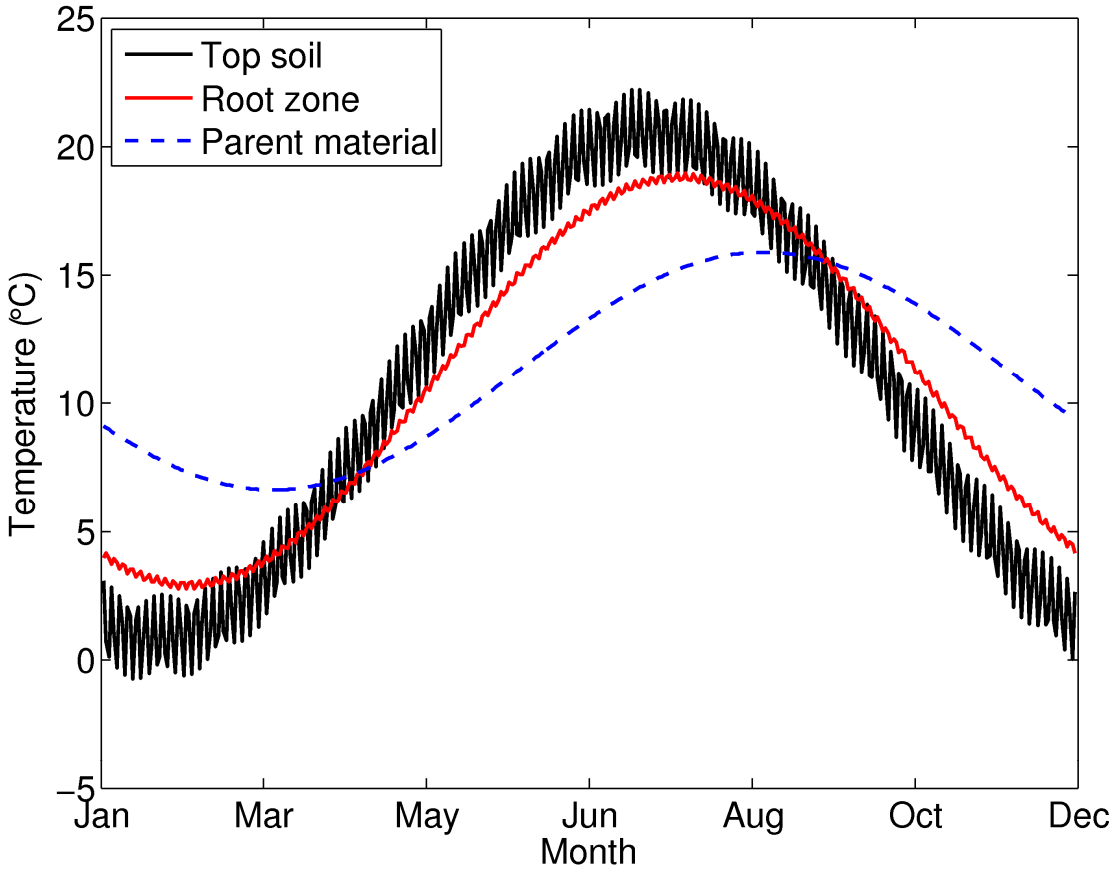
Top soil
Root zone
Parent material
Temperature (°C)
25
20
15
10
5
0
−5
Jan
Mar
May
Jun
Aug
Oct
Dec
Month

Fig. 3.

328

329

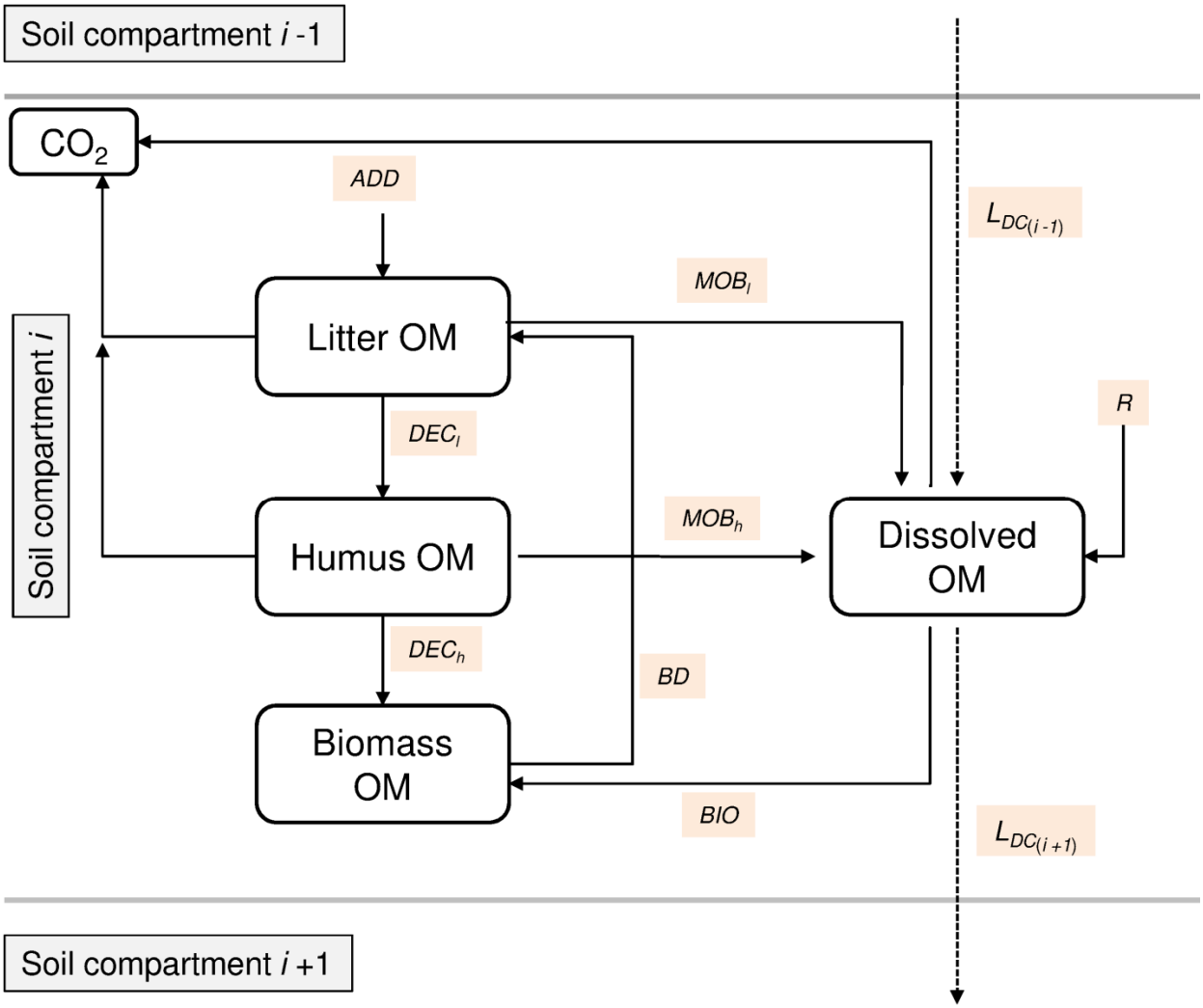

330

331 **Fig. 4.**

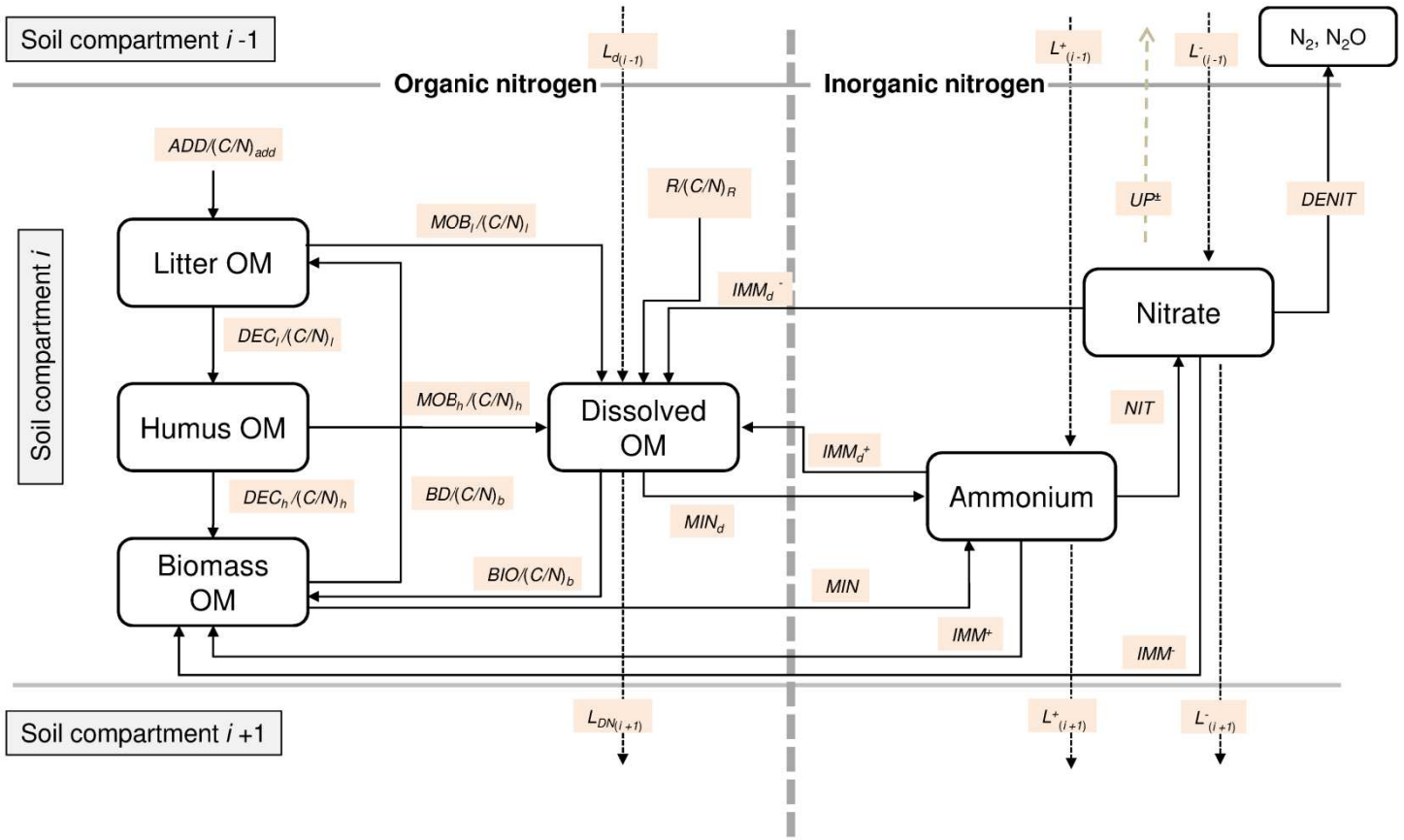
Soil compartment i -1
Organic nitrogen
Inorganic nitrogen
N2, N2O
ADD/(C/N)add
R/(C/N)R
MOBl/(C/N)l
UP±
DENIT
Litter OM
IMMd -
Nitrate
DECl/(C/N)l
Soil compartment i
MOBh/(C/N)h
Dissolved OM
NIT
Humus OM
IMMd+
DECh/(C/N)h
BD/(C/N)b
Ammonium
MINd
Biomass OM
BIO/(C/N)b
MIN
IMM+
IMM-
Soil compartment i +1

Fig. 5.

335

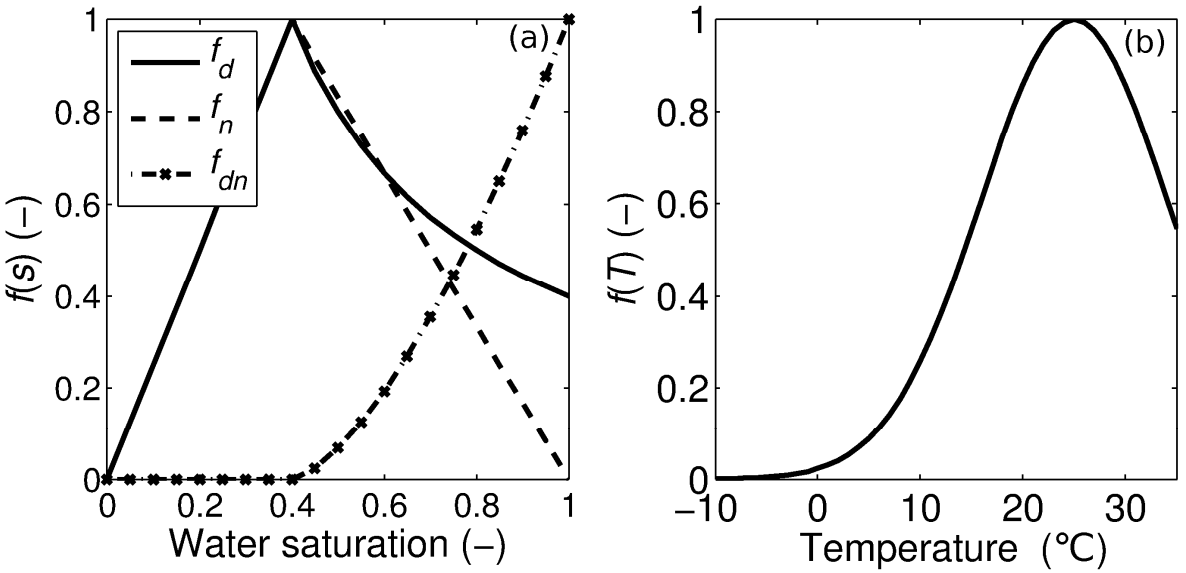

336

337 **Fig. 6.**

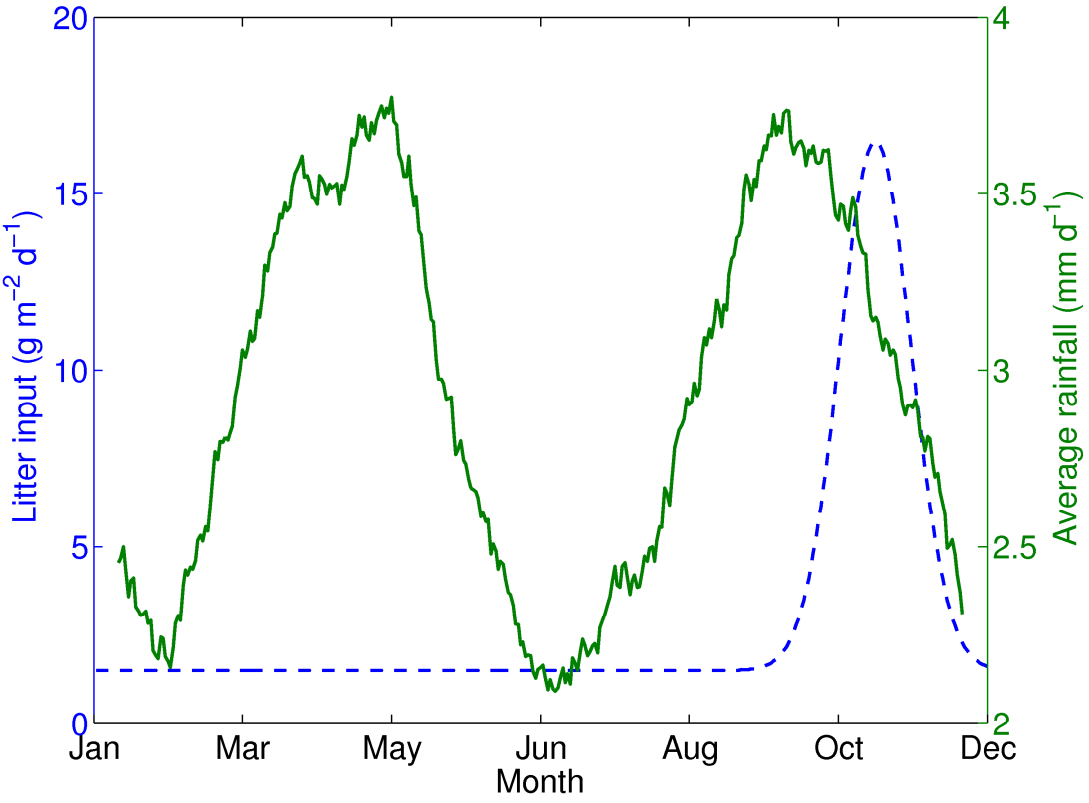
20
15
10
5
0
4
3.5
3
2.5
2
Litter input (g m^{-2} d^{-1})
Average rainfall (mm d^{-1})
Jan
Mar
May
Jun
Aug
Oct
Dec
Month

338

339 **Fig. 7.**

340

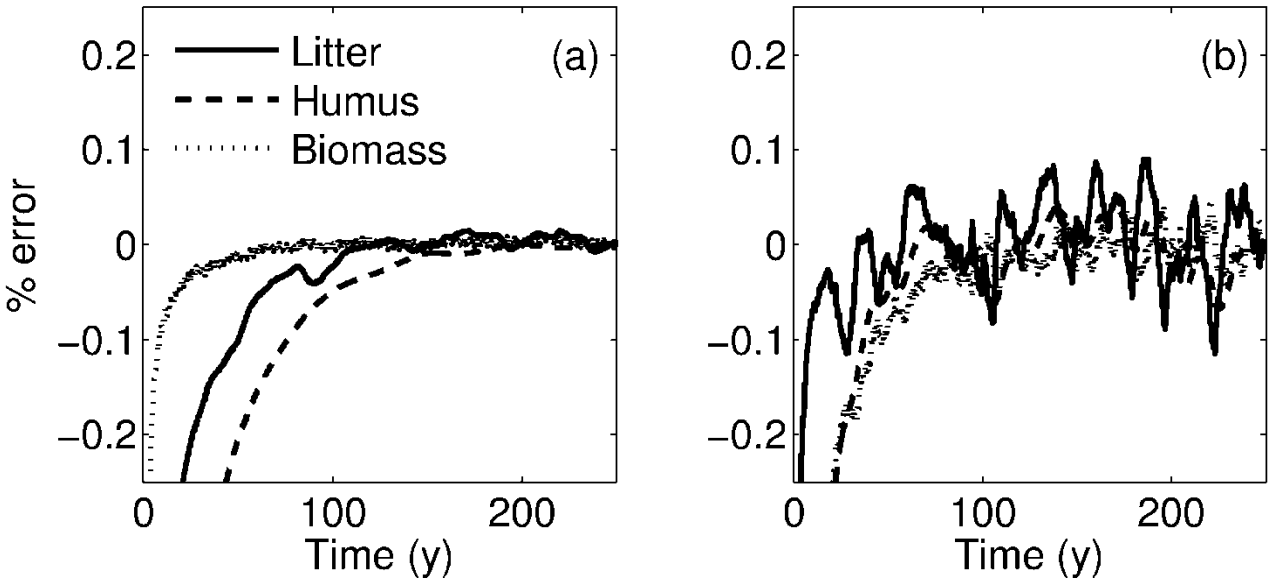

341

342 **Fig. 8**

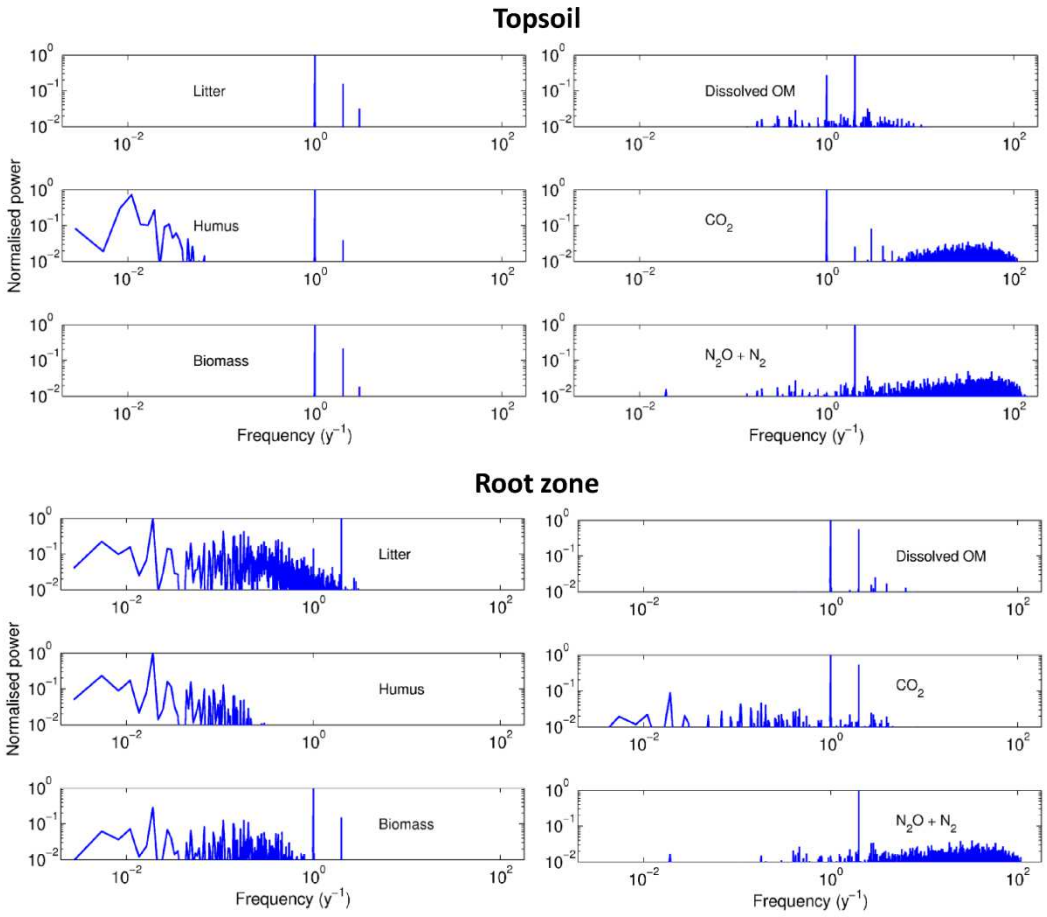
Topsoil
Litter
Dissolved OM
Humus
CO_2
Biomass
$N_2O + N_2$
Normalised power
Frequency (y^{-1})
Root zone
Litter
Dissolved OM
Humus
CO_2
Biomass
$N_2O + N_2$
Normalised power
Frequency (y^{-1})

Fig. 9.